

# REPORT DOCUMENTATION PAGE

AFRL-SR-AR-TR-04-

Public reporting burden for this collection of information is estimated to average 1 hour per response, including the time for reviewing data needed, and completing and reviewing this collection of information. Send comments regarding this burden estimate or any other aspect of this burden to Department of Defense, Washington Headquarters Services, Directorate for Information Operations and Reports (0704-0188). Respondents should be aware that notwithstanding any other provision of law, no person shall be subject to any penalty for failing to comply with a collection of information if it does not have a valid OMB control number. PLEASE DO NOT RETURN YOUR FORM TO THE ABOVE ADDRESS.

0251

ng the  
luding  
02-  
irrently

1. REPORT DATE (DD-MM-YYYY) 10/15/01-2/14/04		2. REPORT TYPE FINAL REPORT		3. DATES COVERED (From - To) 10/15/01-2/14/04	
4. TITLE AND SUBTITLE SYNTHESIS AND CHARACTERIZATION OF POLYIMIDES TO BE USED IN THE FABRICATION OF A LOW DRIVING VOLTAGE ELECTRO-OPTIC MODULATOR				5a. CONTRACT NUMBER F49620-02-1-0014	
				5b. GRANT NUMBER	
				5c. PROGRAM ELEMENT NUMBER	
				5d. PROJECT NUMBER	
6. AUTHOR(S) CONNIE WALTON, Ph.D.  SERGEY SARKISOV, Ph.D.				5e. TASK NUMBER	
				5f. WORK UNIT NUMBER	
				8. PERFORMING ORGANIZATION REPORT NUMBER	
7. PERFORMING ORGANIZATION NAME(S) AND ADDRESS(ES) GRAMBLING STATE UNIVERSITY ALABAMA A & M UNIVERSITY P.O. BOX 881 4900 MERIDIAN STREET GRAMBLING LA 71245 NORMAL ALABAMA 35762					
9. SPONSORING / MONITORING AGENCY NAME(S) AND ADDRESS(ES)					
12. DISTRIBUTION / AVAILABILITY STATEMENT Approve For Public Release: Distribution Unlimited.					
13. SUPPLEMENTARY NOTES					
14. ABSTRACT The aim of this project was to synthesize polyimides that exhibit second order nonlinear optic behavior and to fabricate a Low Driving Voltage Electro-optic Modulator. Undergraduate and graduate students were involved in all aspects of this project. A high temperature polyimide that had a NLO chromophore incorporated was synthesized and its properties characterized. The E-O Coefficient of the polyimide was determined to be 1.98pm/V and expected to have a driving voltage of 9.0 volts. In the detailed analysis of the design of the E-O Modulator Single-arm Interferometer it was determined that the waveguide should have two modes. In the design of the Modulator a new method of coupling light using micro-scratches was tested.					
15. SUBJECT TERMS Polyimides, Nonlinear Optics, Electro-optic Modulator					
16. SECURITY CLASSIFICATION OF:			17. LIMITATION OF ABSTRACT	18. NUMBER OF PAGES 43	19a. NAME OF RESPONSIBLE PERSON Connie Walton, Ph.D.
a. REPORT	b. ABSTRACT	c. THIS PAGE			19b. TELEPHONE NUMBER (include area code) 318-274-6202

20040520 046

# **Final Report**

**for**

**AWARD # F49620-02-1-0014**

**Synthesis and Characterization of Polyimides To Be Used In The  
Fabrication of a Low Driving Voltage Electro-Optic Modulator**

**Grambling State University  
Grambling, Louisiana  
Dr. Connie Walton**

**Alabama A & M University  
Normal, Alabama  
Dr. Sergey Sarkisov**

**April 2004**

**DISTRIBUTION STATEMENT A**  
Approved for Public Release  
Distribution Unlimited

## TABLE OF CONTENTS

<b><i>Part I Synthesis of NLO Materials</i></b>	3
Preparation of aminonitrofluorenone	3
Preparation of N,N dialkylated	6
Preparation of Fluorene Monomer	9
Preparation of N,N Arylated	12
Preparation of Polyimide	14
Nonfluorinated	14
Fluorinated	17
Preparation of Polyamide	18
Summary of Accomplishments	20
 <b><i>Part II Fabrication/Characterization Of electro-optic modulator</i></b>	 21
Waveguide Structure	21
Coupling	22
 Preparation of E/O Polymer films	 24
Characterization of films	25
Summary of Accomplishments	29
 <b><i>References (for Part I &amp; Part II)</i></b>	 41
 <b><i>Part III Presentations/Publications &amp; Students/Staff Involved with Project</i></b>	 42
GSU Student Presentations	42
Presentations given by Dr. Walton	42
GSU Students	42
Publications	43
AAMU Students/Staff	43

The aim of this project was to synthesize polyimides that exhibit second order nonlinear optic behavior and to fabricate a Low Driving Voltage Electro-Optic Modulator. This project was successful in the synthesis/characterization of a fluorene based polyimide, as well as in the design of a single-arm interferometer. Undergraduate and graduate students were involved in all aspects of the project. This three-part final report gives the details of the results obtained. Part I is devoted to the synthesis of the NLO materials, Part II to the fabrication of the Electro-Optic Modulator, and Part III highlights the students that were involved as well as publications/presentations that were given.

## **Part I**

### **Synthesis of NLO materials**

#### Polymer Precursors

##### Aminonitrofluorenone

The synthesis of the fluorene monomer was a three step process. The first step involved selective reduction of 2,7-dinitro-9-fluorenone. This material was purchased from Aldrich Chemical with a purity of 97%. Recrystallizing the dinitro-fluorenone before use optimized the synthesis of 2-amino-7-nitro-9-fluorenone (Figure 1). The recrystallization solvent used was DMF. The purified material was then selectively reduced using NASH [1]. This reducing agent was chosen due to its mild nature. Stronger reducing agents could have reduced both nitro groups as well as the carbonyl group. The crude product was purified by dissolving in DMF and precipitating out using water. The percent yield for this reaction was seventy-one. The structure of the material was confirmed using Infrared Spectroscopy (IR) and Nuclear Magnetic Resonance Spectroscopy (NMR). A solid KBr pellet of the sample was made and analyzed using a Galaxy Matteson FTIR. The spectrum (Figure 2) had an absorption that appears between 3200 and 3500  $\text{cm}^{-1}$ . This absorption is attributed to N-H stretching. The carbonyl group survived the reduction as noted by the peak at 1709  $\text{cm}^{-1}$ . A small amount of the product was dissolved in deuterated acetic acid

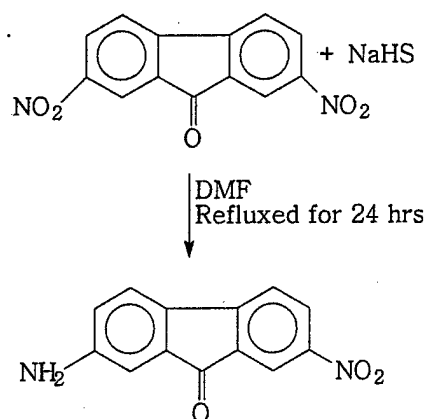


Figure 1  
Synthesis of 2-amino-7-nitro-9-fluorenone

and analyzed using a 270 MHz NMR. The spectrum obtained was consistent with the proposed structure (Figure 3).

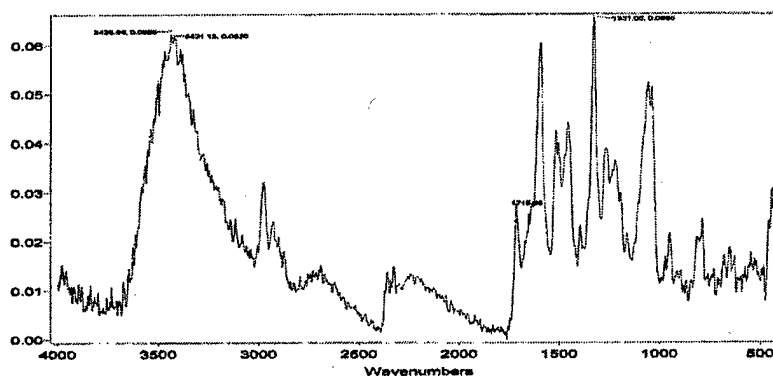


Figure 2  
Infrared Spectrum of 2-amino-7-nitro-9-fluorenone

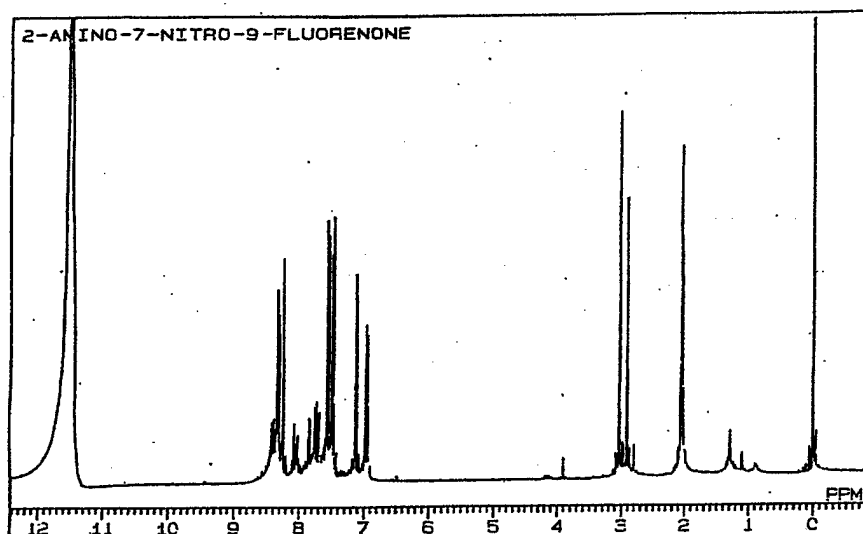


Figure 3  
Proton NMR Spectrum of 2-amino-7-nitro-9-fluorenone

Thermal analysis using Differential Scanning Calorimetry showed a transition that occurred between 230°C and 245°C (Figure 4).

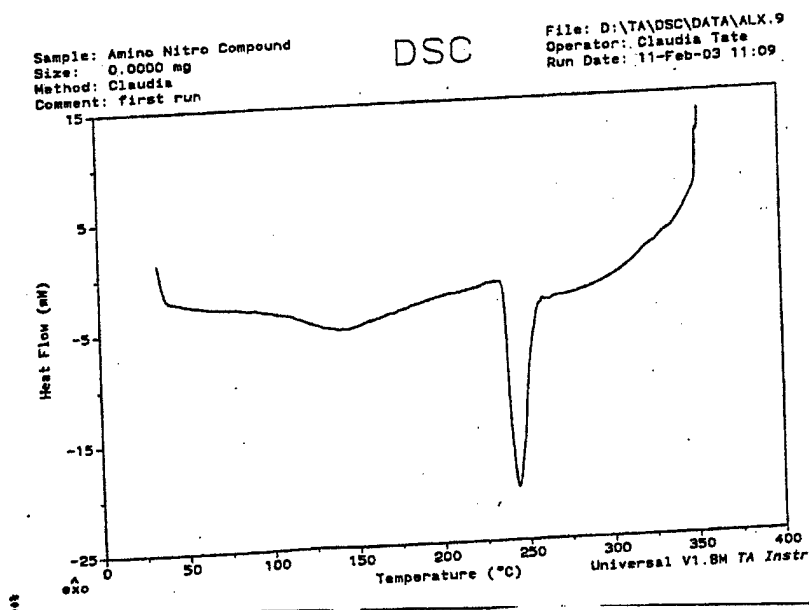


Figure 4  
DSC of Aminonitrofluorenone

The optical properties of 2-amino-7-nitrofluorenone were determined using UV-Vis spectroscopy. The amine was dissolved in dichloromethane and the spectrum was

collected from 200 to 800 nanometers. The compound was found to have absorbencies at 260, 378 and 480 nanometers (Figure 5).

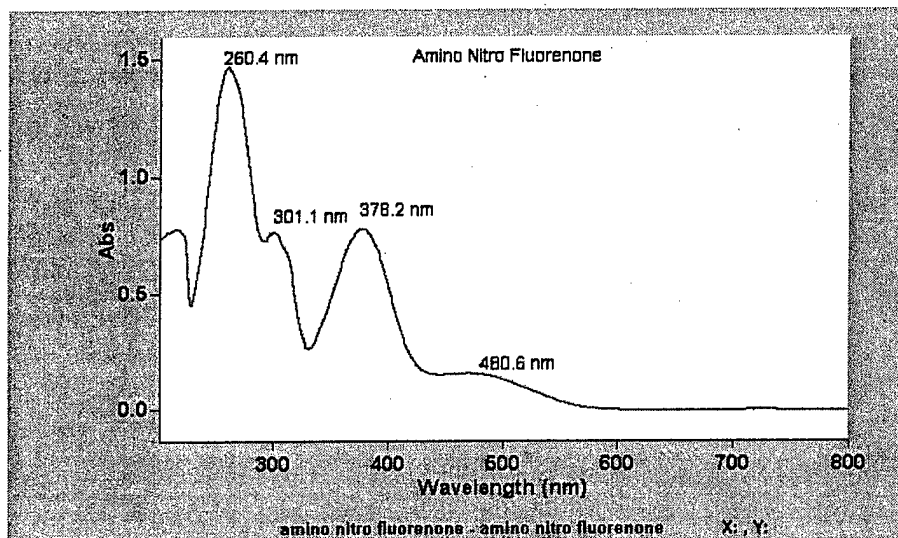


Figure 5  
UV-Visible Spectrum of 2-amino-7-nitro-9-fluorenone

#### N,N dialkylated aminonitrofluorenone

The next step in the synthesis involved increasing the amino nitrogen's donating ability via alkylation. The disadvantage of direct alkylation of amines using alkyl halides lies in stopping the reaction at the desired stage [2]. This results in a complex mixture being formed that consists of the primary amine, secondary amine, tertiary amine, and tetramine. To avoid this complication triethyl phosphate was used as the alkylating agent (Figure 6). The amine was refluxed with excess triethyl phosphate and the reaction monitored using thin layer chromatography. Upon completion of the reaction the excess triethyl phosphate was neutralized using aqueous sodium bicarbonate. The crude material was purified via precipitation from DMF. The percent yield for this reaction was sixty-nine. The material was purified by re-precipitation from DMF.

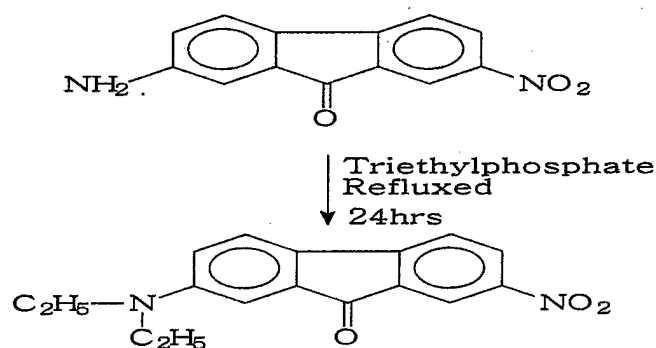


Figure 6  
N,N-dialkylated amino nitro fluorenone

The structure of this compound was confirmed using IR and carbon-13 NMR. The IR spectrum (figure 7) indicates that the N-H bond is no longer present, as noted by the

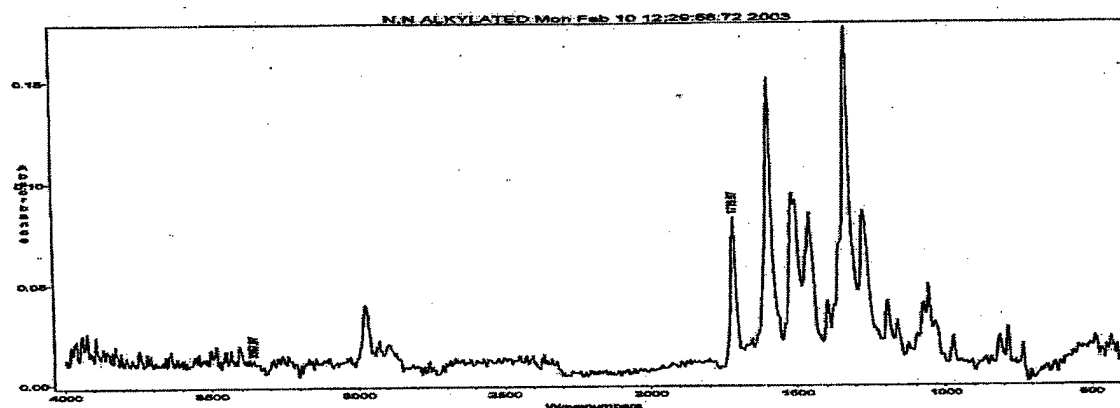


Figure 7  
IR of N,N diethylaminonitrofluorenone

absence of N-H stretching. This is consistent with the behavior for tertiary amines. The Carbon-13 spectrum (Figure 8) has peaks present that represent the carbons that have different environments. The UV-Vis spectrum for this compound showed absorbencies at 290, 417 and 540 nanometers (Figure 9).

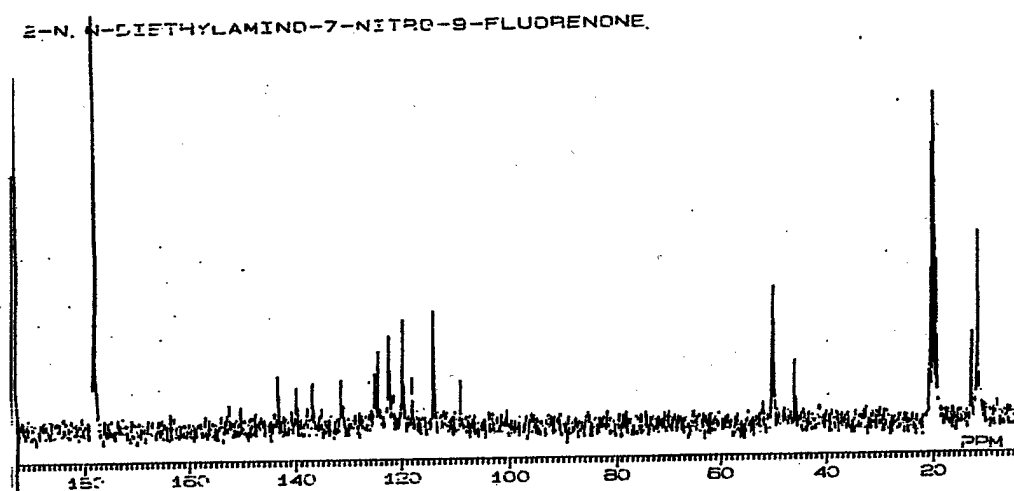


Figure 8  
Carbon-13 NMR of N,N diethylaminonitrofluorenone

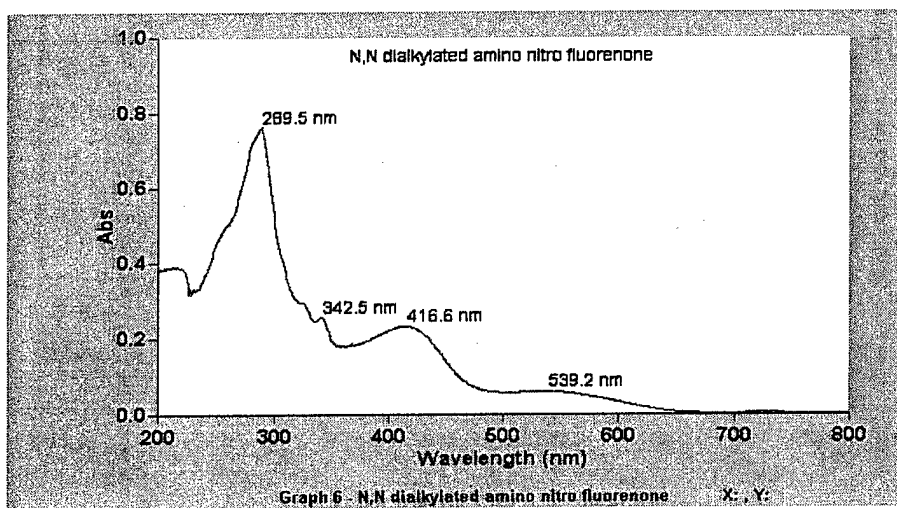


Figure 9  
UV-Visible Spectrum of N,N-diethylaminonitrofluorenone

Thermal analysis using DSC showed an absorbance between 150° and 200°C (Figure 10).

Sample: N,N-alkylated  
Size: 0.0000 mg  
Method: Alex  
Comment: first run

DSC

File: D:\TA\DSC\DATA\ALX.6  
Operator: Alex Lodge  
Run Date: 4-Feb-03 14:06

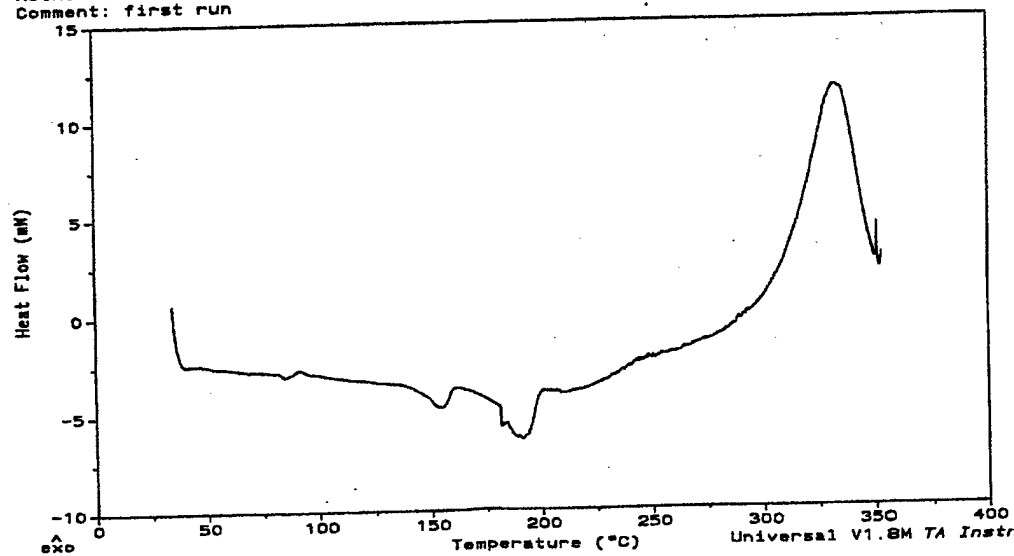


Figure 10  
DSC thermogram of N,N diethylaminonitrofluorenone

### Fluorene Monomer

The procedure used for the preparation of the monomer (Figure 11) was analogous to the procedure employed by Scanlon to produce p,p'-Diaminodiphenylmethane [3]. The N,N -dialkylated amine was refluxed for twenty-four hours with an excess of aniline under acidic conditions. The pH of this reaction was critical to the overall yield of the product. An acidic environment was necessary to minimize the formation of a Schiff base as a side product (figure 12). A reaction was done in which the pH was approximately 2.

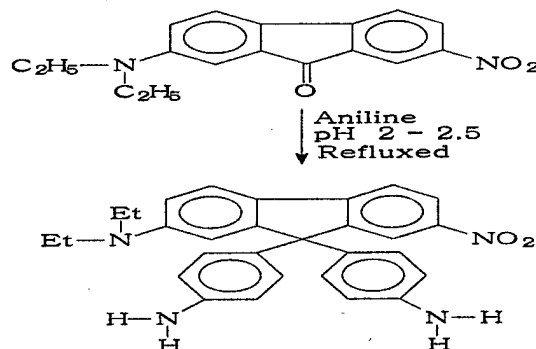


Figure 11  
Synthesis of Fluorene Monomer

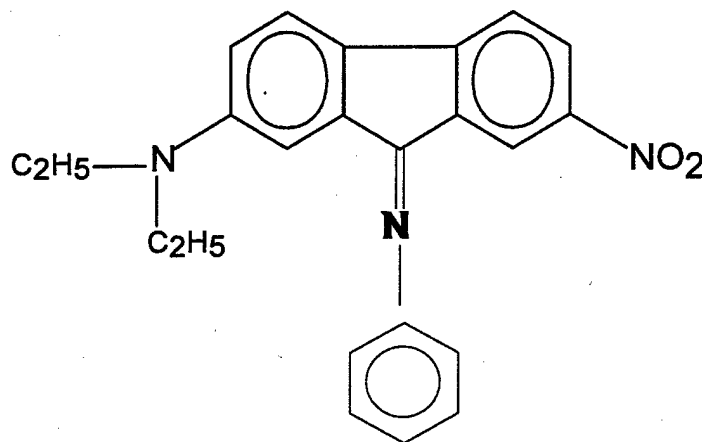


Figure 12  
Schiff Base formed as Side-Product

Upon work-up of the reaction a material was obtained that was insoluble in all solvents, including DMF. Under these conditions the compound was apparently degraded. Another reaction was conducted in which the pH was 4.0. The reaction was worked-up by neutralizing the solution. The product was obtained via extraction, using ethyl acetate as the solvent. The product was isolated by dripping the ethyl acetate solution into hexane. The material obtained was a tar. The tar was dissolved in methanol and then slowly dripped into water. A reddish-orange powder was obtained in a percent yield of fifteen. An IR spectrum was obtained (figure 13) and indicated that N-H stretching was present. The monomer structure was also confirmed using proton NMR (Figure 14). The UV-Vis spectrum of the monomer showed absorbencies at 270nm and 450nm (Figure 15). The thermal behavior of the monomer was determined using differential scanning calorimetry (DSC) and thermogravimetric (TGA) analysis. The DSC showed an exotherm at 110°C and an endotherm at 320°C (Figure 16). TGA analysis indicated a significant weight loss at temperatures above 300°C. This weight loss is most likely due to degradation of the compound.

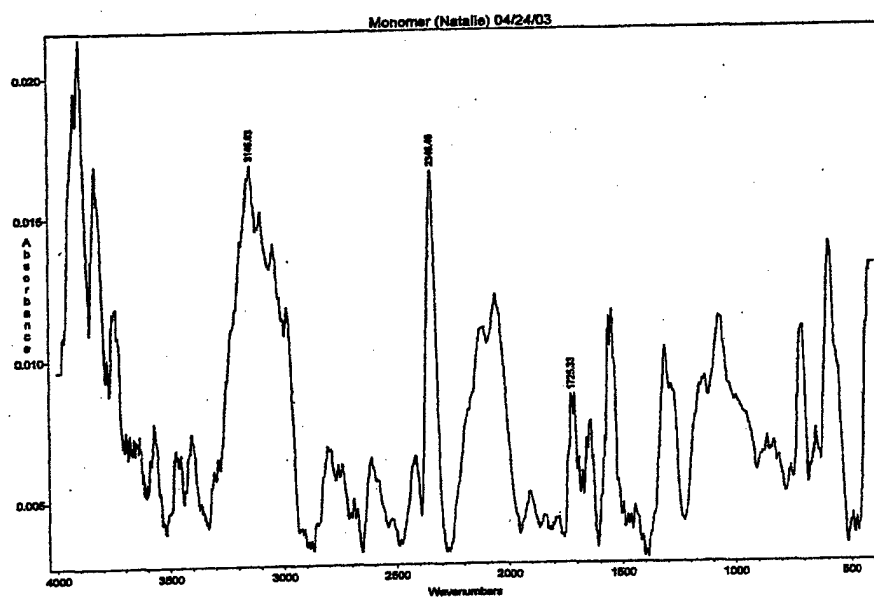


Figure 13  
Infrared Spectrum of Fluorene Monomer

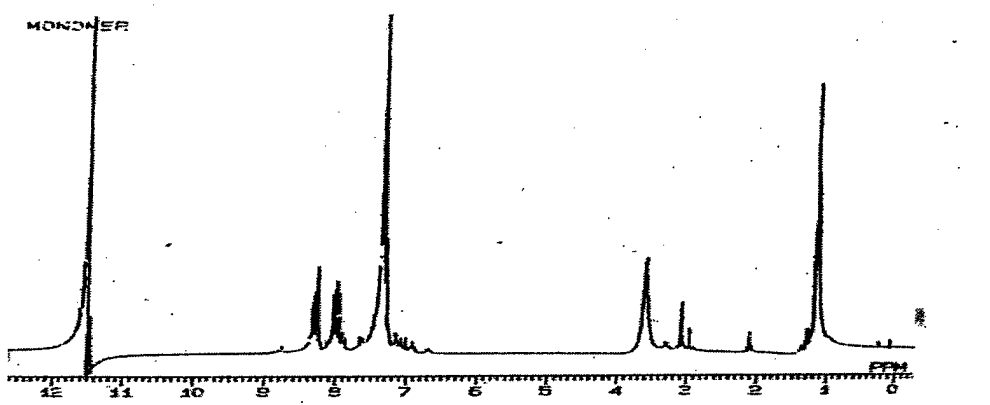


Figure 14  
Proton NMR of Fluorene Monomer

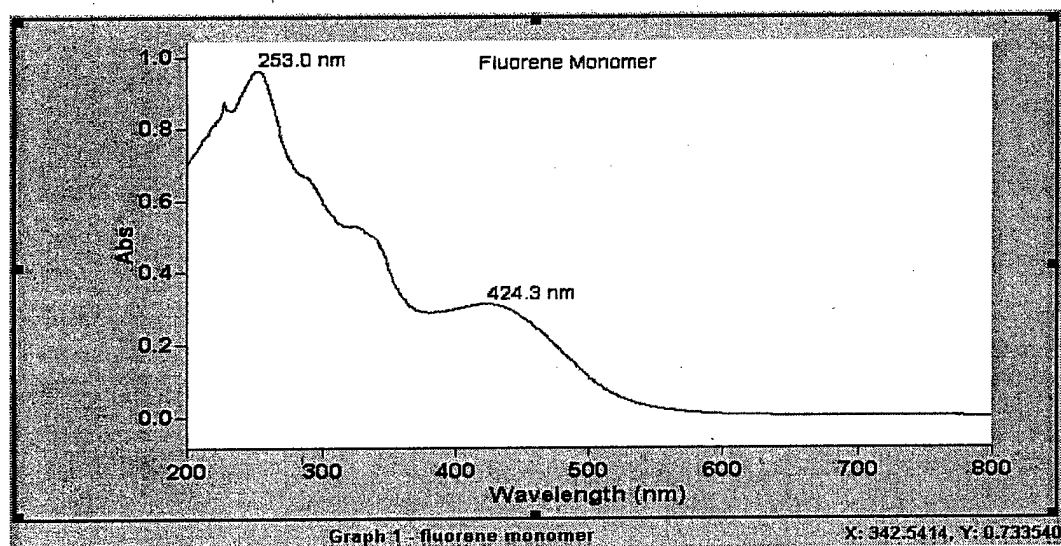


Figure 15  
UV-Visible Spectrum of Fluorene Monomer

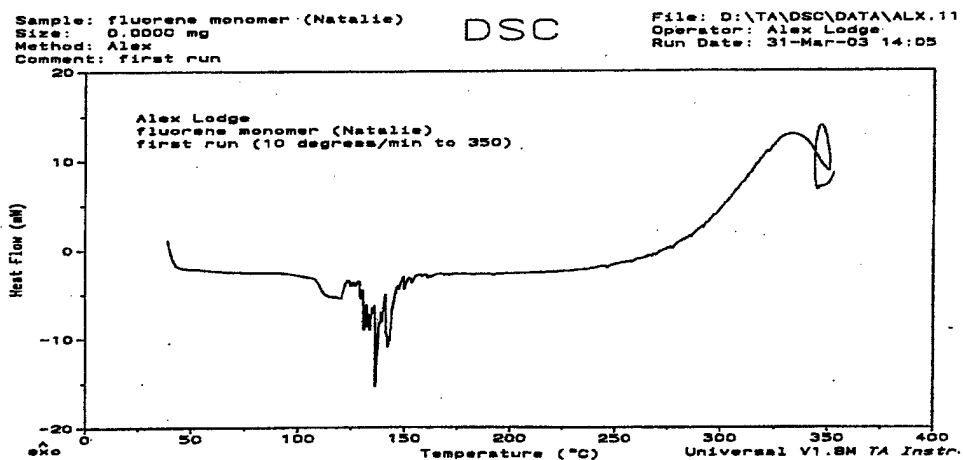


Figure 16  
DSC of Fluorene Monomer

### N,N Arylated aminonitrofluorenone

An attempt was made to further increase the donating ability of the amine by replacing the ethyl groups on N, N-diethylaminonitrofluorenone with thiophene groups (Figure 17). Research has shown that the replacement of alkyl groups with aromatic groups significantly increases the conjugation of a molecule and therefore increases the dipole

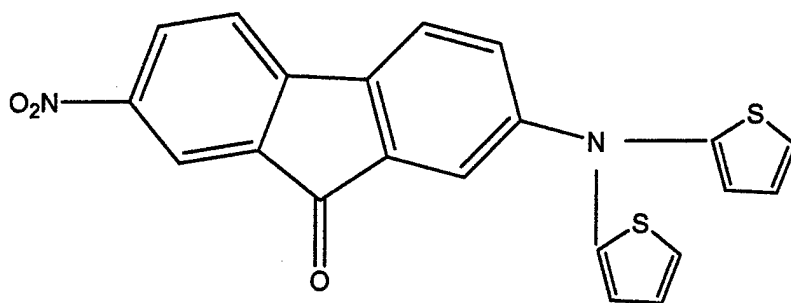


Figure 17

### N,N Arylated Fluorene Derivative

moment. The aminonitrofluorenone was reacted with iodothiophene in the presence of 18-Crown-6 and potassium carbonate. The solvent for this reaction was dichlorobenzene. The reaction was monitored using thin layer chromatography and stopped after 36 hours. The product was isolated, purified, and obtained in 24% yield. Analysis of the product via IR (Figure 18) and melting point analysis seemed to indicate that starting material was recovered. It was thought that this was due to the fact that the starting aminonitrofluorenone had limited solubility in dichloromethane. As a result the reaction was repeated using dimethyl formamide as the solvent. The percent yield for the crude product was fifty-six. This material is being purified by column chromatography.

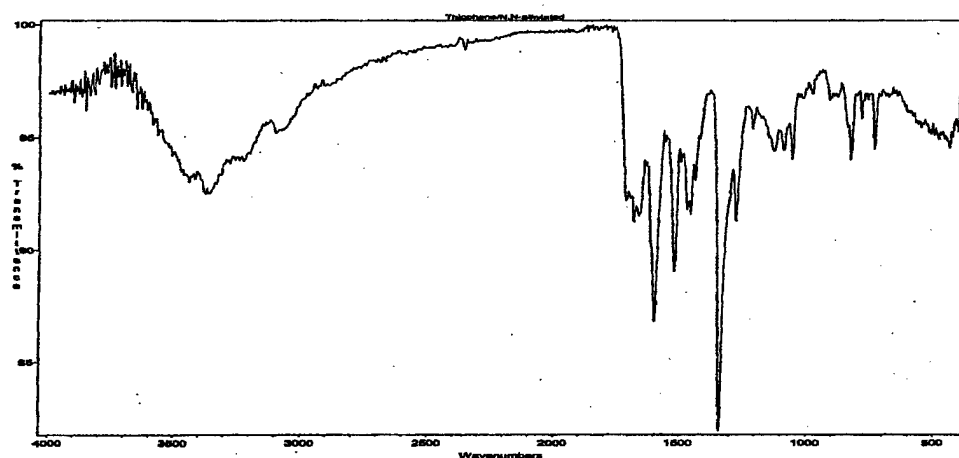


Figure 18

IR spectrum of material isolated in Thiophene derivative synthesis

### Preparation of Polyimide

In the polymerization of the fluorene monomer with benzophenone tetracarboxylic acid dianhydride an attempt was made to find synthesis conditions that would result in the isolation of a soluble polyimide. As a result a procedure reported by Moy and McGrath [4] was followed. This procedure involved converting the dianhydride into a diester, thus eliminating the sensitivity to moisture realized with anhydrides. The polymerization was conducted at a temperature of 160°C for 16 hours. The material obtained was the Polyamic acid (figure 19). Unreacted monomer was removed from the polyamic acid by

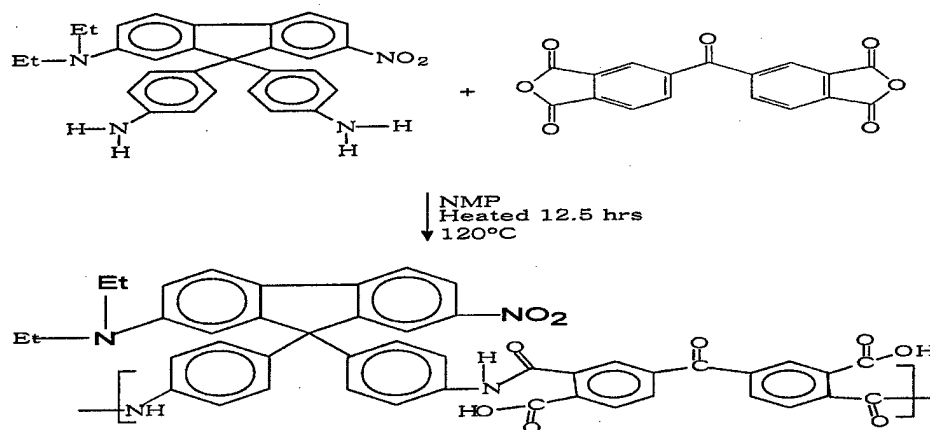


Figure 19  
Synthesis of Polyamic Acid

washing the material with methanol with the aid of a blender. The Polyamic acid was dried in a vacuum oven at 45°C and analyzed using IR and DSC. The Infrared Spectrum (Figure 20) had absorbances present due to N-H stretching and O-H stretching. Two glass transitions were observed in the DSC chromatogram of the polymer (Figure 21). The first T<sub>g</sub> was believed to be due to the polyamic acid. The second transition was attributed to the presence of polyimide. The presence of the polyimide can be explained in two possible ways. The first is the polyimide was formed during the polymerization reaction, which was conducted at a temperature of 120°C. Another option is during the DSC analysis as the temperature increased imidization occurred. The polyimide (figure 22) was obtained by thermally annealing the polyamic acid at 120°C for 24 hours in a

vacuum oven. The polyimide was found to be insoluble in organic solvents, not behaving like the polyimides reported by Moy. This insolubility presented a problem in that thin films that were needed for optical property determination could not be made. It was thought that the high reaction temperature that was used in the formation of the polyamic acid resulted in the isolation of a material that had already started to undergo extensive imidization. The thermal annealing of this material produced a polymer that had extensive imidization. In an effort to enhance the solubility of the polyimide

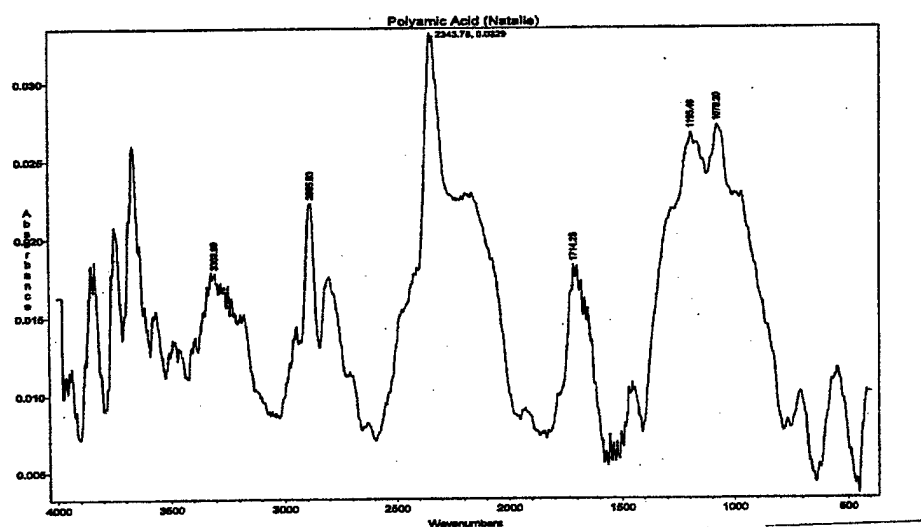


Figure 20  
IR of Polyamic Acid

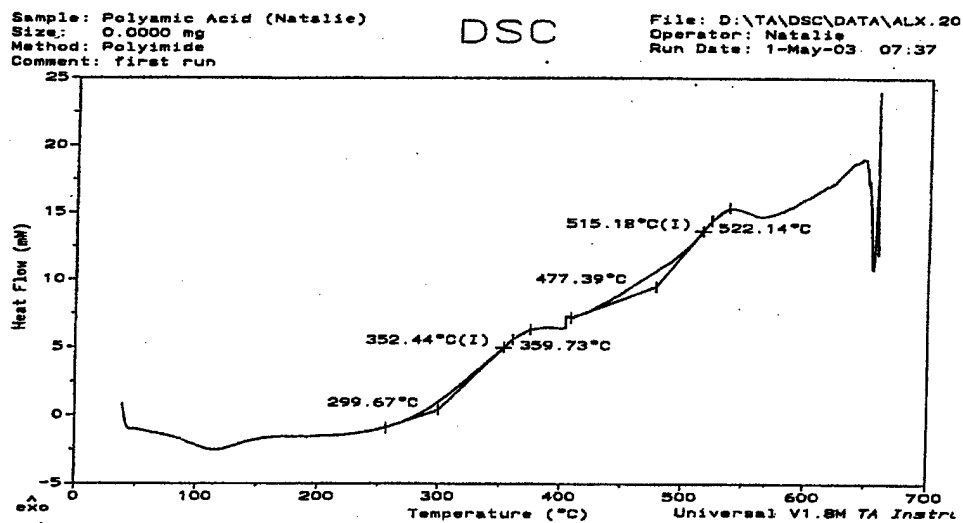


Figure 21  
 DSC of Polyamic Acid

the polymerization was repeated using a lower temperature, 120°C. The polyamic acid obtained was soluble in DMF and dichlorobenzene. It was converted to the polyimide (Figure 22) via thermal annealing.

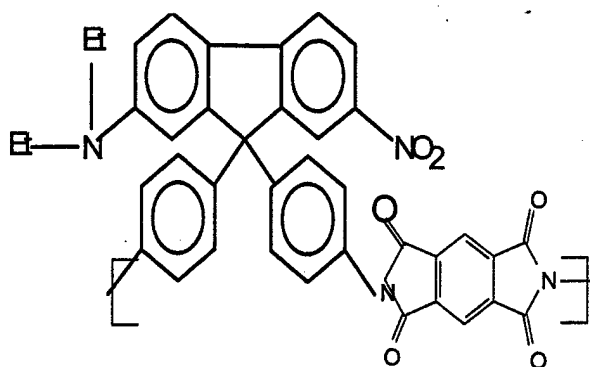
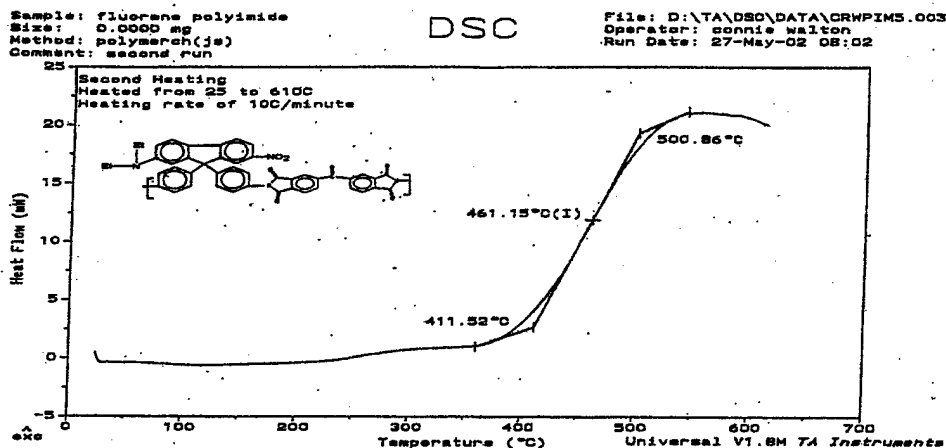


Figure 22  
 Fluorene Polyimide

The resulting polyimide had a Tg of 460°C (Figure 23) and was also insoluble in organic solvents.



*DSC of polyimide formed between fluorene monomer and benzophenone tetracarboxylic dianhydride.*

Figure 23  
DSC of Polyimide

A decision was made to provide Dr. Sergey Sarkisov, physic professor at Alabama A & M, with polyamic acid samples. This was done in an effort to support the formation of films. Once the polyamic acid films were made thermal annealing would support the conversion into the polyimide.

#### Fluorinated Polyimide

A polyimide was synthesized using a fluorinated dianhydride, 4,4'-(Hexafluoroisopropylidene)diphthalic anhydride (figure 24). The presence of the fluorine groups in the structure appeared to destabilize the product slightly. Thermally

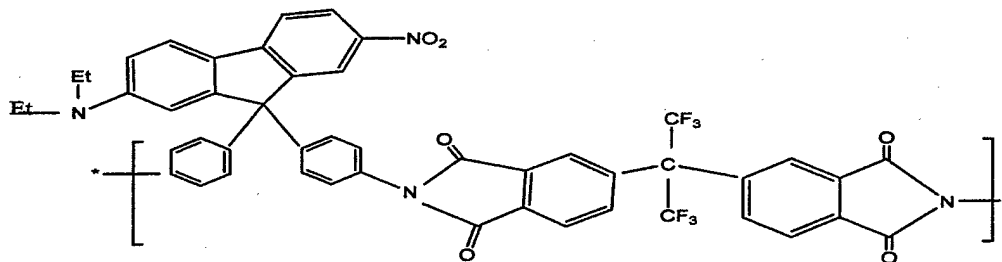


Figure 24  
Fluorinated Polyimide

annealing the polyamic acid, appeared to slightly degrade the product. This was indicated by the presence of black specks embedded in the sample. This reaction was repeated a number of times, all of which resulted in a product that appeared to be partly decomposed. The glass transition temperature of this material was obtained, and found to be slightly above 400°C (figure 25).

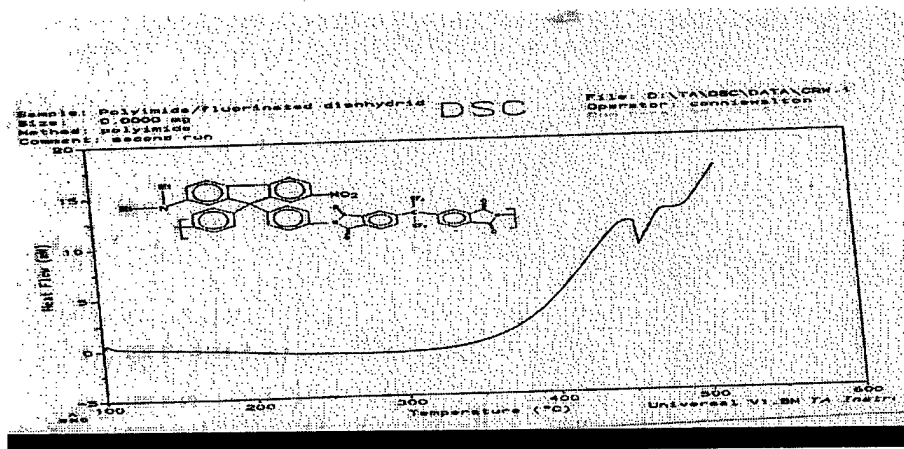


Figure 25  
DSC of Fluorinated Polyimide

### Polyamide

The polyamic acids that were synthesized were sent to Dr. Sergey Sarkisov for NLO analysis and ultimately incorporation into an Electro-Optic Modulator. These materials presented solubility difficulty in the preparation of solutions needed for thin films. The ideal solvent for use is one that has a low vapor pressure. In solvents such as these the polyamic acid had limited solubility. As a result, a polyamide (Figure 26) was synthesized to address the solubility issue.

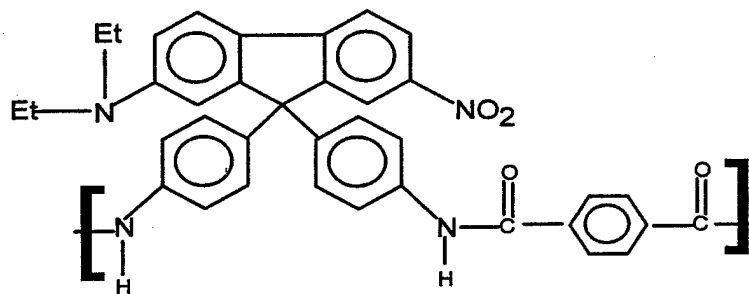


Figure 26  
Polyamide Synthesized

The fluorene monomer was reacted with an equal molar amount of terephthaloyl chloride using dimethylformamide as the solvent. Care was taken to ensure that the reaction was

free of water. The polymer was isolated by dripping the reaction mixture into water. The polyamide was purified further by dissolving in DMF and precipitating using water. The Polymer was analyzed using Infrared Spectroscopy. N-H stretching is observed between  $3500\text{ cm}^{-1}$  and  $3200\text{ cm}^{-1}$ (figure 27). The amide I peak, which is due to carbonyl stretching, appears at approximately  $1700\text{ cm}^{-1}$ . The amide II peak, which is due to N-H bending appears at approximately  $1680\text{ cm}^{-1}$ . The thermal behavior of this polymer was analyzed using DSC (figure 28). Two glass transitions are observed ( $250^{\circ}\text{C}$  and  $350^{\circ}\text{C}$ ). This is probably due to the polymer sample isolated being polydisperse.

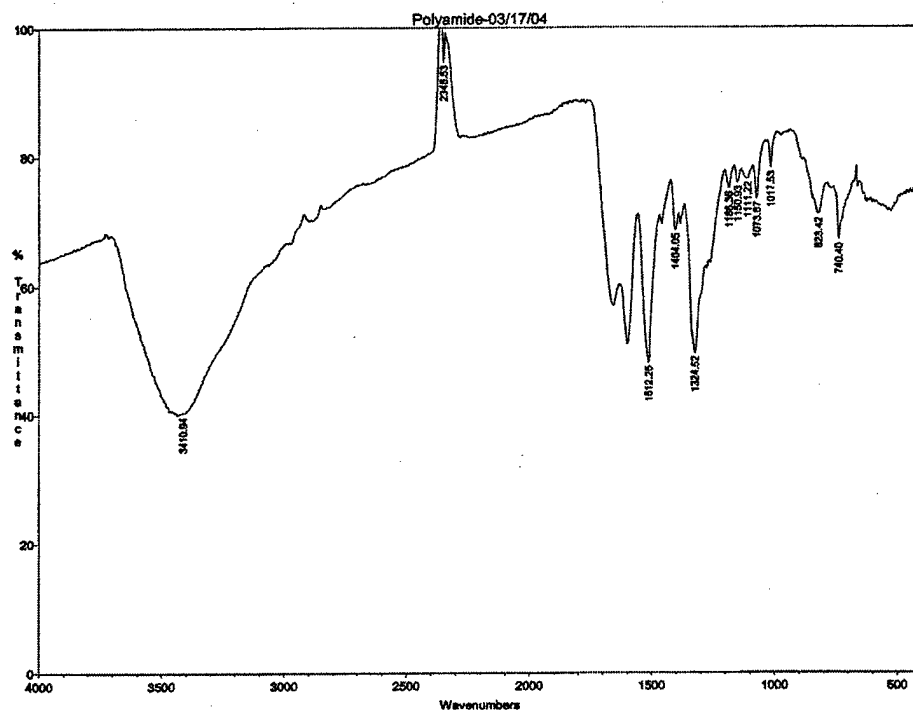


Figure 27  
IR of Polyamide

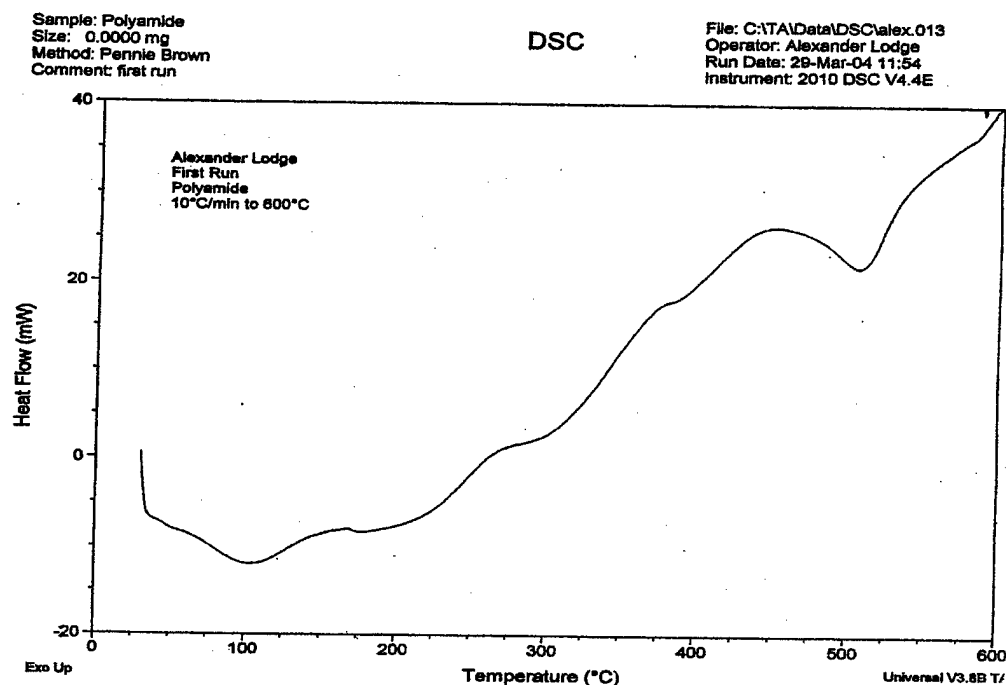


Figure 28  
DSC Thermogram of Polyamide

### **SUMMARY OF ACCOMPLISHMENTS**

- Synthesized and characterized Monomer precursors
- Optimized synthesis of Monomer
- Synthesized and characterized Polymer precursors
- Synthesized two different Polyimides (fluorinated & nonfluorinated)
- Optimized Synthesis of Polyimides
- Characterized Thermal Behavior of Polyimides
- Via trial and error identified synthetic steps that can be used to Arylate the Aminonitrofluorenone
- Synthesized and characterized a Polyamide
- Undergraduate students involved in this project developed organic synthesis techniques

## Part II

### Fabrication and characterization of the electro-optic modulator

#### 1. Design

##### 1.1. Waveguide structure

It has been shown in Year 1 Report that a planar waveguide electro-optic (E-O) modulator that exploits the interference of two co-propagating modes of different orders can be characterized by the half-wave voltage  $V_\pi$

$$V_\pi = \frac{\lambda_0 d_{eff}}{R n_e^3 r_{33} L}, \quad (1)$$

where  $\lambda_0$  is the wavelength of light,  $d_{eff}$  is the effective thickness of the waveguide,  $n_e$  is the extraordinary refractive index of the E-O polymer film,  $r_{33}$  is the E-O coefficient of the film,  $L$  is the travel distance of the light within the film between the electrodes,  $R$  is the factor depending on the parameters of two modes of different order used in the interferometer. The modulator will be comparable to standard Mach-Zehnder in terms of driving voltage, if factor  $R$  could be made close to 1.0. This puts certain requirements for the modes of the waveguide that are discussed below.

Figure 29 shows the detailed schematic of the multi-layer structure of the modulator used as an example of the approach. The structure consists of a fused quartz substrate coated with conductive ITO coating. A buffer layer of silica ( $\text{SiO}_2$ ) is built over the ITO film. The next layer is the E-O polymer film. It is covered with the second buffer layer made of Norland 65 UV curable adhesive (in case of the high temperature E-O polyimide it must be replaced with silica). On the top of the second buffer layer we have ITO film. The refractive index of the ITO films was measured using the prism coupling technique. The refractive index (real part of the complex index for a conductive coating) is 1.819, and the thickness is approximately 0.21  $\mu\text{m}$ . Buffer layers isolating waveguide core from ITO electrodes are necessary. Otherwise, traveling mode will escape from the core into ITO layer with high real component of the refractive index and will quickly decay there due to high imaginary component of the index. The separation between the polymer core and the electrodes has to be sufficient to prevent leaking of the propagating modes and, on the other side, should not be too large for the driving voltage to remain

low. The other concern is the thickness of the polymer core. The proposed design uses two propagating modes simultaneously in a single-arm interferometer. Factor  $R$  gets closer to 1.0 when the indices of modes  $TM_0$  and  $TM_1$  vary differently with the change of the index of the film  $n_f$ . We found out that this condition will be well satisfied if the thickness of the core will be such that it can support only two modes  $TM_0$  and  $TM_1$  with near-critical (cut-off) condition for the second mode. In this case index of mode  $TM_0$   $N_0$  will vary slow in response to the change of  $n_f$  while index of mode  $TM_1$   $N_1$  will have a very sharp change. As a result, parameter  $\delta N_{01} = \delta(N_0 - N_1)$ , variation of the difference between the indices of the modes, will vary rapidly in response to the electric field induced variation of the index of the film ( $n_f = n_e$  in our case)  $\delta n_f$ . This approach is illustrated in Figure 30 for a core made of commercial E-O polymer LD-3 from AdTech Systems Research, Inc. The refractive index of the polymer was measured to be 1.689 (at 633 nm). If the core is 0.48- $\mu\text{m}$  thick (Figure 30a), both parameters  $\delta N_0$  and  $\delta N_{01}$  change with almost the same rate as  $\delta n_f$  increases ( $\delta n_f = 0$  when the index is equal to 1.689). Factor  $R$  associated with the rate is close to one. When the core is 0.87- $\mu\text{m}$  thick (Figure 30b), it now supports three modes and parameter  $\delta N_{01}$  changes with low rate ( $R$  is less than 0.1). Correspondingly, it brings up undesirable increase of the half-wave voltage (Eq. (1)) due to low  $R$ . This shows an importance of maintaining the optimum thickness of the waveguide core in order for the proposed modulator to compare favorably against the Mach-Zehnder interferometer. In order to evaluate the half-wave voltage of the E-O modulator (Eq. (1)), we took  $\lambda_0 = 633$  nm,  $L = 25.4$  mm,  $n_e \approx 1.689$ ,  $r_{33} = 11$  pm/V (LD-3), the effective thickness  $d_{eff} = d + d_{b1} + d_{b2} = 3.48$   $\mu\text{m}$  ( $d = 0.48$   $\mu\text{m}$ , thickness of the first buffer layer  $d_{b1} = 2.0$   $\mu\text{m}$ , thickness of the second buffer layer  $d_{b2} = 1.0$   $\mu\text{m}$ ),  $R \approx 1$ . This set of parameters gives  $V_\pi = 1.63$  V, a low voltage that indicates the compatibility of the modulator with standard silicon-based electronic circuitry.

## 1.2. Coupling

We initially proposed a new approach to coupling light with planar waveguide structure of the E-O modulator based on incorporation of high-index coupling prisms into substrate (see Year 1 Report). However, we have encountered technological problems

that could not be resolved within the time frame of the project and the funds available. The incorporation of the coupling prisms was done by attaching them to the side faces of a thick (~6 mm) substrate made of fused silica with optical adhesive. Then the top faces of the substrate and the attached prisms were polished in order to make a smooth uniform surface for spin casting of the light guiding film. However, there was a 100- $\mu\text{m}$  wide gap between the face of prism and the adjacent side face of the substrate filled up with the adhesive. This gap created conditions of reflection of polymer solution being spin cast during the process of film deposition. As a result, we could not obtain a uniform polymer film carrying light from the point of coupling at the prism to the region over the substrate where actual waveguide structure was built. In this technological approach the gap could not be eliminated because a certain amount of adhesive had to be there in order to hold firm prism and substrate together. Some other techniques, without use of adhesive, had to be used for the integration of the coupling prisms. However it goes beyond the scope of this project.

We explored an alternative approach to coupling light with a planar waveguide structure of the E-O modulator that needs no coupling prisms or rather expensive diffraction gratings fabricated by the photolithographic process. The idea of the approach is somehow similar to the principle of coupling with a diffraction grating incorporated into planar waveguide. The explanation is given in Figure 31. Two scratches, input and output, are made in a thin film planar waveguide. The incident light beam strikes the input scratch (Figure 31a). Scratch can be considered as a wideband spatial disturbance generating rich spectrum of spatial wave vectors  $k_s$  (Figure 31b). There is always a possibility to find a wave vector  $k_s$  in this "reservoir" that, being combined with the horizontal component of the wave vector of the incident light wave  $k \sin \theta$  ( $\theta$  is the angle of incidence), will satisfy the matching condition for the wave vector of the waveguide traveling mode  $k_m$  (Figure 31c)

$$k_s + k \sin \theta = k_m . \quad (2)$$

As a result, some portion of the energy of the incident light beam will be transferred to the waveguide mode. The reverse process occurs in the output scratch. The energy of the mode is transferred to the light beam propagating in free space.

Experimental testing of the approach was conducted with a waveguide made of a thin film of polymer poly(methyl methacrylate) known as PMMA on pre-oxidized silicon wafer (thickness of the layer of silicon dioxide was  $1.5\text{ }\mu\text{m}$ ) as shown in Figure 32. The waveguide had two TE and TM propagating modes. The light was successfully coupled with and decoupled from the waveguide using two scratches made by a razor blade cutting through the polymer film. Efficiency of coupling/decoupling was estimated using the input scratch and the decoupling prism. The total throughput of the waveguide depicted in Figure 32 (including coupling losses in the scratch, losses in the waveguide, and the losses of decoupling in the prism) was  $2.5 \times 10^{-4}$  for TE modes and  $1.0 \times 10^{-4}$  for TM modes. The coupling efficiency for TE modes turns out to be 2.5 times greater.

## 2. Preparation of electro-optic polymer films

Fabrication of polymer films was done using spin casting technique. Conductive metal coating was made using DC magnetron sputtering. In order to add to thin film of polymer electro-optic properties corona poling technique was used as described in Year 1 report. Three types of corona poling apparatus were designed and fabricated. The first one, based on a grid of corona wires, was described in Year 1 report. It was used to pole in air films of commercial E-O polymer LD-3 from AdTech Systems Research, Inc. with glass transition temperature  $T_g$  that did not exceed  $150^\circ\text{C}$ . Since the heating in the first apparatus was done by drawing electric current through the conductive ITO coating on a glass substrate where the polymer film was placed, it was impossible to use the system for corona poling of polyimide films. They required heating to a temperature of nearly  $500^\circ\text{C}$ . At this temperature the glass substrates usually cracked. The second system was designed and built with a powerful external heater and a corotron with a needle and a bias grid. The films of polyimide from Grambling State University were spin cast on ITO coated quartz disks (at 750 rpm, 1000 rpm, 2000 rpm, and 3000 rpm). Disk was placed on the top of the heater of the corona poling apparatus. Electric contact was made between ground and the ITO coating of the substrate. Then the apparatus was placed in a chamber filled with argon. The voltage on the needle was kept at 13 kV. The voltage on the bias grid was  $\sim 500\text{V}$ . The temperature of the sample during corona poling was kept near  $500^\circ\text{C}$ . The corona poling was conducted for 3 hours at constant temperature. Then the

heater was turned off and the corona poling was conducted while the sample was cooling down to room temperature. There was an apparent change of the color of the films after heating. The initially reddish films turned brown. No E-O effect was detected in these films. Optical absorption spectroscopy of the films (Figure 33) indicated that the absorption peak near 440 nm attributed to the E-O chromophore incorporated in the polymer molecule disappeared after heating. This was clear indication of the decomposition of the chromophore at the temperature of poling. The presence of argon did not prevent the chromophore from destruction.

Then an alternative corona poling technique without heating was used. The third corona poling apparatus was designed and fabricated. The apparatus did not have heater and was mounted on a hot plate kept at a temperature of 50°C. It had a needle and a bias grid. Samples of polyimide film were spin cast on ITO coated glass substrates. Sample was inserted inside apparatus right after spin casting. The corona was turned on. One sample was made without bias grid. The voltage on the needle was 13 kV. Corona current reached 40  $\mu$ A. Corona poling was performed for 8 hours while the solvent was slowly drying off from the film. The distance from the needle to the film was 28 mm. Corona current damaged the region in the film and substrate right under the needle. The circular region of the film around the damaged area turned brown. We did not detect any E-O effect in this brown circular region. The brown color could be again attributed to the decomposed E-O chromophore. Other samples were poled with the bias grid present. We applied voltage of the order of 560 V to it. The voltage on the needle was 15 kV. The corona current was between 1.3 and 1.7  $\mu$ A. The process lasted for 8 hours while the film was dried after spin casting. Reference sample of commercial material LD-3 (voltage on the bias grid was 560 V) was also poled in the same way. This sample did not exhibit any E-O effect. The film of polyimide did demonstrate E-O effect. Then the control sample of polyimide was made by drying without corona poling. It also demonstrated relatively strong E-O effect of the second order.

### 3. Characterization of the electro-optic polymer films

Characterization of the E-O coefficients of polymer films was conducted using the reflection method proposed in Reference 5. Experimental setup is presented in Figure

34. Incident light beam polarized at an angle of  $45^\circ$  with respect to the plane of incidence passes through the substrate, transparent layer of ITO, and polymer film. Then it gets reflected from a chromium electrode deposited on the top of the polymer film. Reflected beam passes through a Soleil-Babinet compensator, cross-polarized analyzer and enters photo detector. An alternating voltage from a signal generator is applied to the polymer film between ITO (grounded) and chromium electrodes. Signal generator sends reference signal to a lock-in amplifier. Signal from the photo detector is also sent to the lock-in. Signal after filtering in the lock-in is sent to an oscilloscope.

When the alternating voltage is applied to the polymer film, it changes its ordinary and extraordinary refractive indices  $n_o$  and  $n_e$  due to the E-O effect. This correspondingly changes the optical path length of  $s$  and  $p$  polarized components of the beam. As a result, the elliptically polarized reflected beam experiences the change of its ellipse of polarization induced by the alternating voltage. When the reflected beam passes through the cross-polarized (with the plane of polarization oriented perpendicular to the polarization plane of the incident beam) analyzer, the time variation of the ellipse of polarization results in the time variation of the intensity of the beam. This time varying intensity produces periodic signal the amplitude of which is measured by lock-in amplifier. Soleil-Babinet compensator is used to change the elliptic polarization of the reflected beam and thus the intensity of the beam passing through the analyzer. Two sets of data must be collected. One set refers to the d.c. intensity of the output beam when no alternating voltage is applied. For the lock-in to be used for measurements of the output intensity, a chopper is used to chop the incident light beam. The output intensity is plotted versus the position of the compensator. The intensity should periodically change from maximum (when the reflected beam is linearly polarized along the direction of the analyzer) to zero (when the reflected beam is linearly polarized across the direction of the analyzer). The half-maximum d.c. intensity  $I_c$  is the parameter that should be extracted from this data. Another set of data is obtained when the alternating voltage is "ON". Now the amplitude of the periodic intensity of the output beam is plotted versus the position of the compensator. It also periodically changes from maximum to minimum when the position of the micrometer screw of the compensator changes. The amplitude of this

periodical variation  $I_m$  is the parameter that should be extracted from this data. The E-O coefficient  $r_{33}$  of the polymer film ( $r_{33} = 3 r_{31}$ ) can be calculated as [1]

$$r_{33} = \left( \frac{I_m}{I_c} \right) \frac{3\lambda_0}{4\pi V_m} \frac{(n^2 - \sin^2 \theta)^{3/2}}{n^2 (n^2 - 2 \sin^2 \theta) \sin^2 \theta}, \quad (3)$$

where  $V_m$  is the amplitude of the alternating voltage;  $n$  is the refractive index of the polymer film ( $n \approx n_0$ );  $\theta$  is the incidence angle (in our case it was  $45^\circ$ ).

The technique was used to measure E-O coefficients of reference materials such as LiNbO<sub>3</sub> and corona poled commercial polymer LD-3, and of the films of polyimide synthesized at GSU. The reflecting chromium film with a thickness of approximately 100 nm was made using d.c. magnetron sputtering. Experimental data for a 0.2-mm thick plate of LiNbO<sub>3</sub> (coated with ITO and chromium on opposite sides, no substrate was used) is presented (Figure 35) in the form of plots of d.c. intensity and amplitude of the modulated intensity versus the position of the screw of the Soleil-Babinet compensator (proportional to actual phase shift between horizontally and vertically polarized components of the incoming elliptically polarized light). Parameters  $I_c$  and  $I_m$  are shown by arrows in the plots. These parameters were used to calculate E-O coefficient  $r_{33}$  of the plate. Parameters  $V_m$  and  $\theta$  were 14 V and  $45^\circ$  respectively. The refractive index  $n = n_0 = 2.286$ . The estimated coefficient  $r_{33} = 116.41$  pm/V turned out to be 3.78 times greater than the highest E-O value  $r_{33} = 30.8$  pm/V reported in the literature [6]. The reason for that could be experimental error or other E-O effects, which are not related to the Pockels effect. In Ref. 1 the interference of the beams reflected from both sides of the E-O layer was mentioned as a factor of error. Correction factor 3.78 was assumed to be valid for the experimental setup. In order to obtain realistic estimate for the E-O coefficient, the experimentally extracted value had to be divided by this factor.

Experimental results for commercial polymer LD-3 are presented in Figure 36. The film of polymer solution in cycloheptanone (as described in Year 1 report) was spin cast on an ITO coated glass substrate at 650 rpm for 120 s. No cross-linker was added. Then it was baked in open air for 2 hours at  $80^\circ\text{C}$ . Corona poling was done in the first corotron (see Year 1 report). The high voltage on corona wires was 9 kV, the bias voltage on the grid was 150 V. Higher bias voltage produced intense "frost" deformation of

surface of the polymer that scattered light. The film was kept at a temperature of  $150^{\circ}\text{C}$  during corona poling for 1 hour. Then the heater was turned off and the film cooled down to room temperature while the corona was "ON". After the film was poled, 100-nm thick chromium electrode was deposited on it. The measurement of the E-O coefficient was done ten days after poling. Evaluation of the E-O coefficient  $r_{33}$  of the film using data in Figure 36 gave a value of 7.98 pm/V for the E-O coefficient. The true E-O coefficient was estimated using the correction factor. It turned out to be  $r_{33} \approx 2.1$  pm/V, value about 5 times less than 11 pm/V (at a wavelength of 1.3  $\mu\text{m}$ ) reported by the manufacturer as the figure-of-merit of the material [7]. The sample was checked again three months after poling. It was stored at room temperature. The sample did not exhibit any detectable E-O effect. Thermal relaxation of the ordered orientation of the E-O chromophore added to polymer molecule more likely contributed to this effect.

Experimental results for the polyimide synthesized at GSU are presented in Figure 37. The sample was prepared by spin casting of polyimide solution in gamma-butyrolactone (as described in Year 1 report) on an ITO coated glass substrate at 1000 rpm for 120 s. Then it was placed in the corotron of the third type and corona poled while drying at  $50^{\circ}\text{C}$ . The high voltage on the needle of the corotron was 14.5 kV, the bias voltage on the grid was 549 V. Corona current was initially 1.6  $\mu\text{A}$  and then dropped down to 1.3  $\mu\text{A}$ . The total time of poling/drying was 8 hours. The oscillogram of real modulation signal obtained from the sample is presented in Figure 38. The experimental results in Figure 37 were used to evaluate the effective E-O coefficient of the film equivalent to the coefficient of linear E-O effect. For parameters  $V_m = 10\text{V}$ ,  $n=n_{TE}=1.7148$ , and  $\theta = 45^{\circ}$  Eq. (3) gave a value of 7.47 pm/V for the E-O coefficient. The true value (obtained with the use of the correction factor) was estimated as  $r_{33} \approx 1.98$  pm/V, E-O coefficient sufficiently high to expect driving voltage of the planar waveguide modulator close to 9.0 V (see sub-section 1.1).

Figure 39 shows the amplitude of the signal proportional to the varying intensity of light reflected by the sample of poled polyimide film versus the amplitude of the alternating voltage. The dependence is apparently linear, which might serve as additional evidence of the true linear E-O (Pockels) effect in the corona poled polyimide.

As was mentioned above, quadratic E-O effect was also observed in polyimide film prepared at the same conditions but without simultaneous poling. In this case the E-O effect was due to mechanism other than the Pockels effect. It could possibly be the deformation of the film due to electric force of attraction between electrodes, which is proportional to the square of the applied electric field.

#### **Summary of accomplishments**

1. Literature search and vendor survey was conducted
2. Personal contacts were established
3. Detailed analysis of the design of the E-O modulator in the configuration of single-arm interferometer was done. The waveguide should have two modes, and the sub-critical cut-off conditions must be maintained for the second order mode. In this case the driving voltage approaches 1.63 V.
4. New method of coupling light with planar waveguide E-O modulator was proposed and successfully tested. The method uses micro-scratches in the waveguide as the means of coupling. The method replaces initially proposed technique of integration coupling prisms with the substrate. Implementation of this approach requires additional resources.
5. Three corona poling methods and devices were designed and used for poling polymers studied in the project.
6. Experimental set-up for characterization of the E-O coefficients of polymers was designed, built up, and tested.
7. Characterization of E-O coefficients was conducted. The polyimide synthesized by Dr. Walton at GSU, polymer of interest in the project, did exhibit linear E-O effect. The E-O coefficient of the polyimide was estimated to be 1.98 pm/V. The expected driving voltage of the E-O modulators based on polyimide film was estimated as 9.0 V.
8. Three students, one M.S. and two Ph.D., received training through participation in the project.

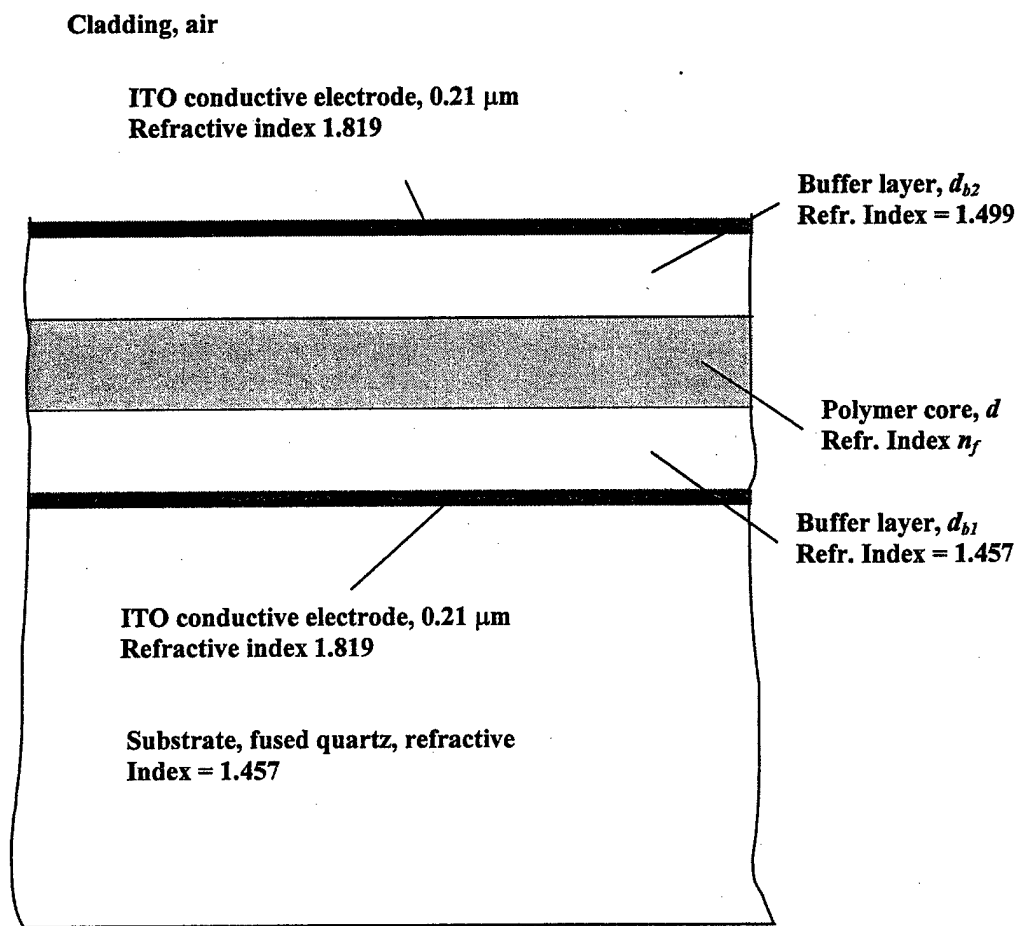


Figure 29. The schematic of the multi-layer structure of the waveguide E-O modulator

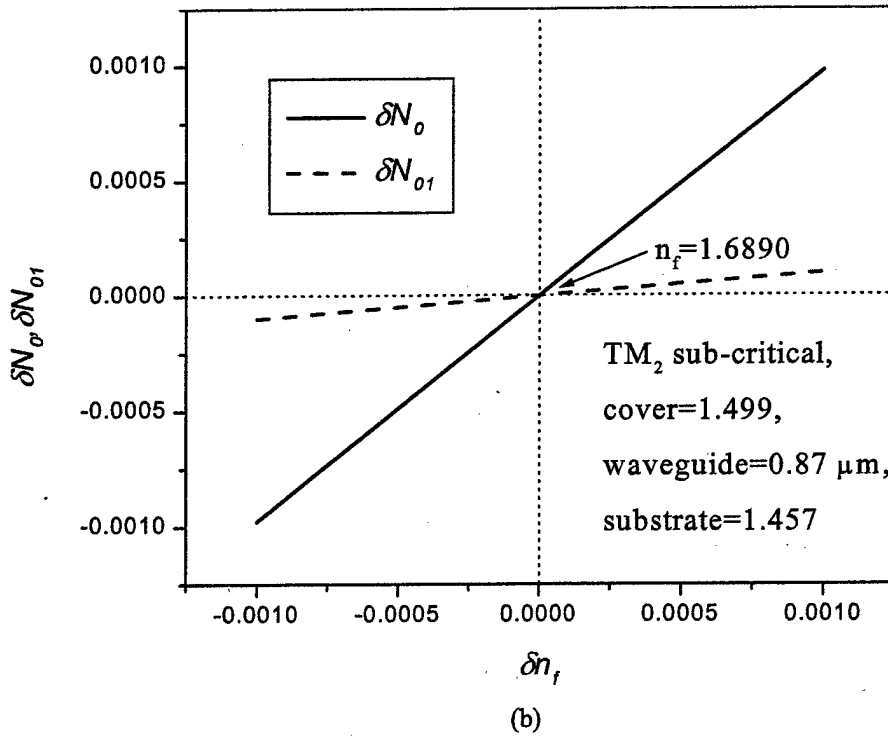
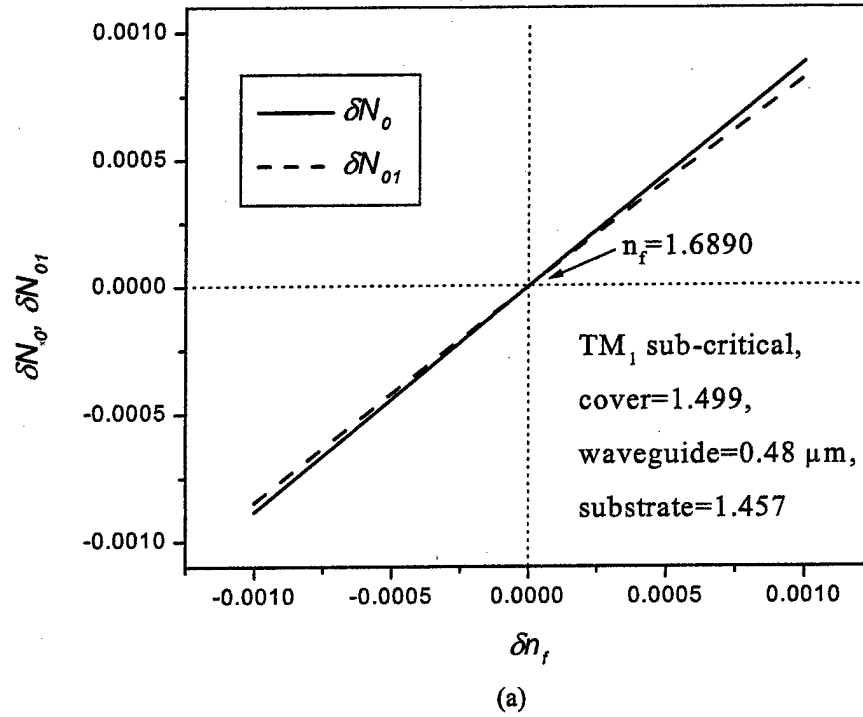
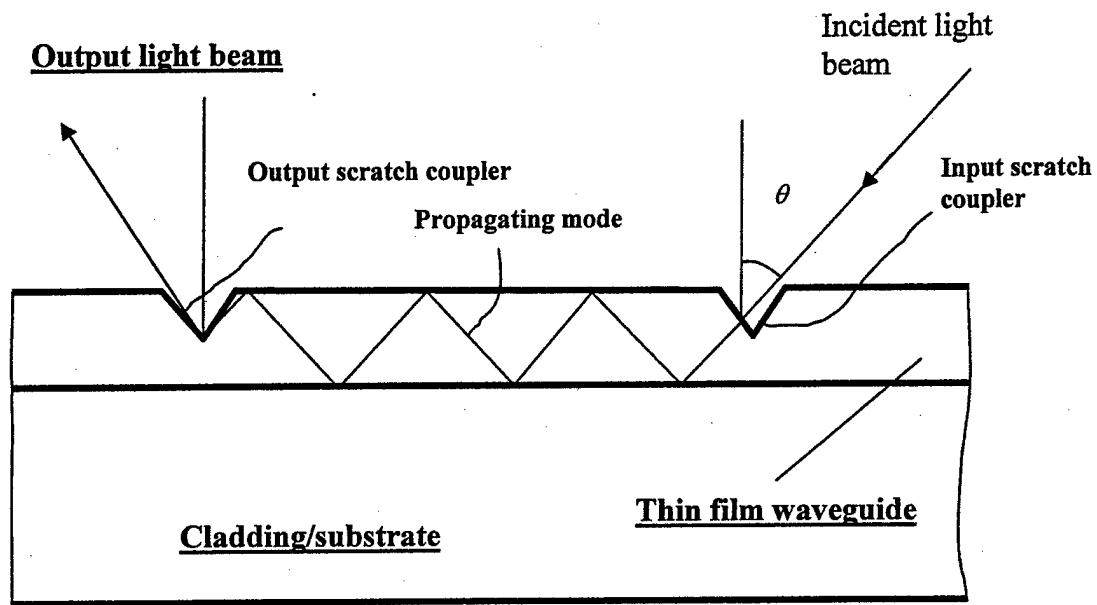
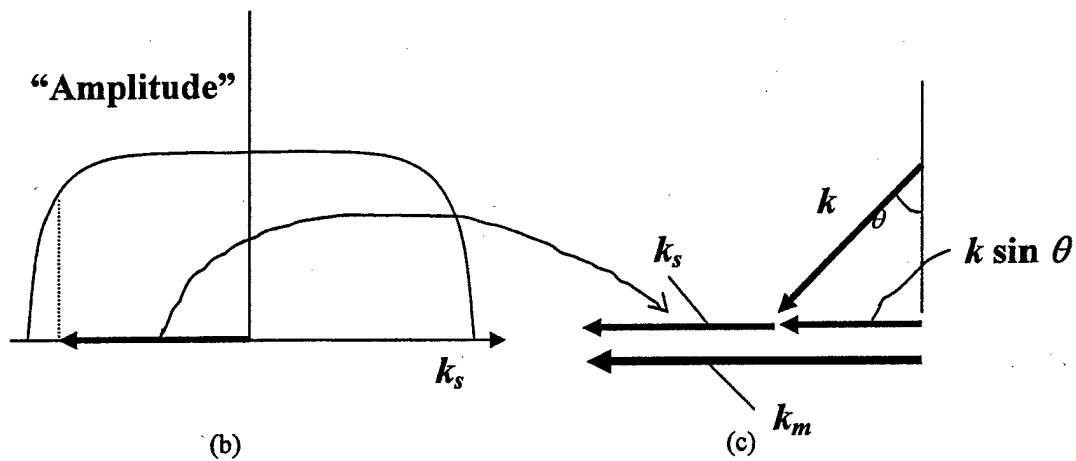


Figure 30. Parameters  $\delta N_0$  and  $\delta N_{01}$  plotted versus the variation of the film refractive index  $\delta n_f$  for (a) the waveguide core supporting two propagating modes (sub-critical condition for TM<sub>1</sub>) and for (b) the waveguide supporting three modes (sub-critical condition for TM<sub>2</sub>). The waveguide core material is E-O polymer LD-3 with refractive index 1.689 (at 633 nm).



(a)



(b)

(c)

Figure 31. (a) Structure of the "scratch" waveguide couplers; (b) Spectrum of wave vectors generated by the scratch coupler; (c) matching conditions for wave vectors of the incident wave coming from free space  $k$ , wave vector of the scratch  $k_s$ , and the waveguide traveling mode wave vector  $k_m$ .



Figure 31. Photograph of the traveling mode in a polymer waveguide generated by beam from a He-Ne laser coupled with a waveguide using scratch coupler (on the right). Bright spot on the left corresponds to the output light decoupled from the waveguide using output scratch coupler.

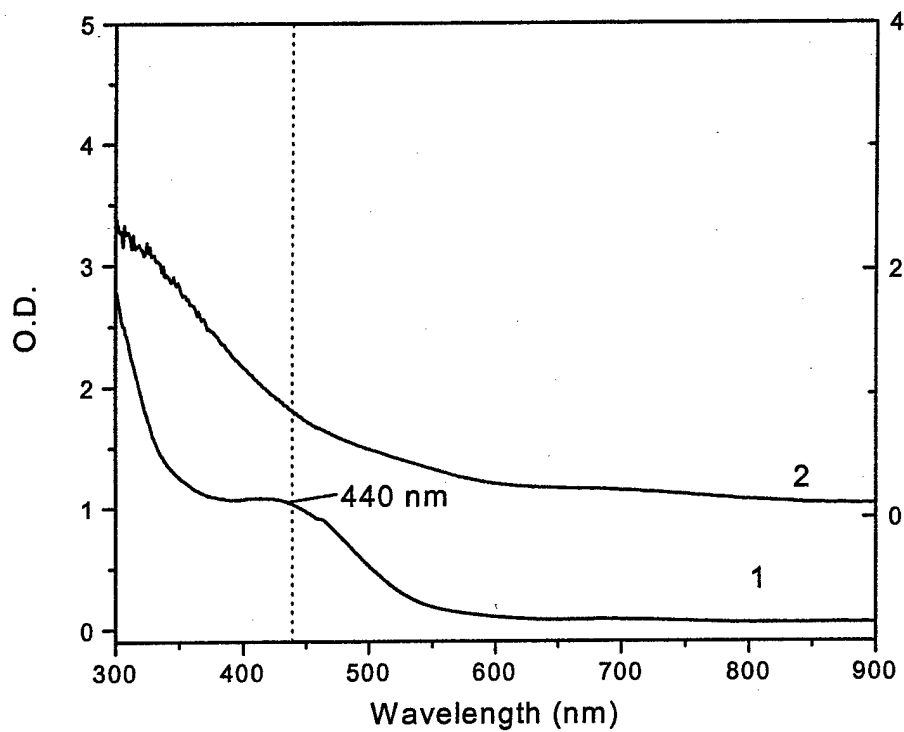


Figure 33. Optical absorption spectrum of the polyimide film (1) before heating and (2) after heating at 500°C for 3 hours in argon.

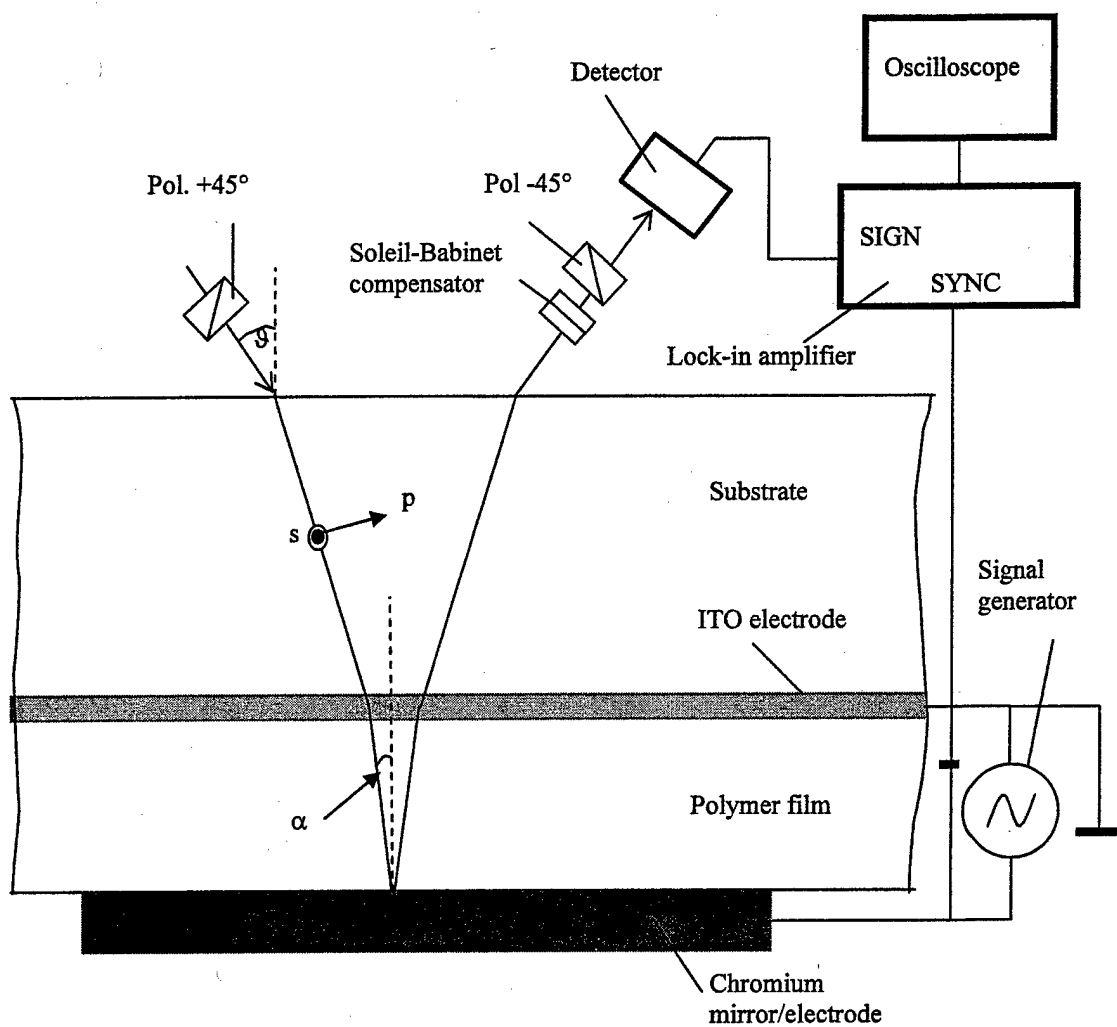


Figure 34. Experimental setup for characterization of E-O coefficients of polymer films proposed in Ref. 1.

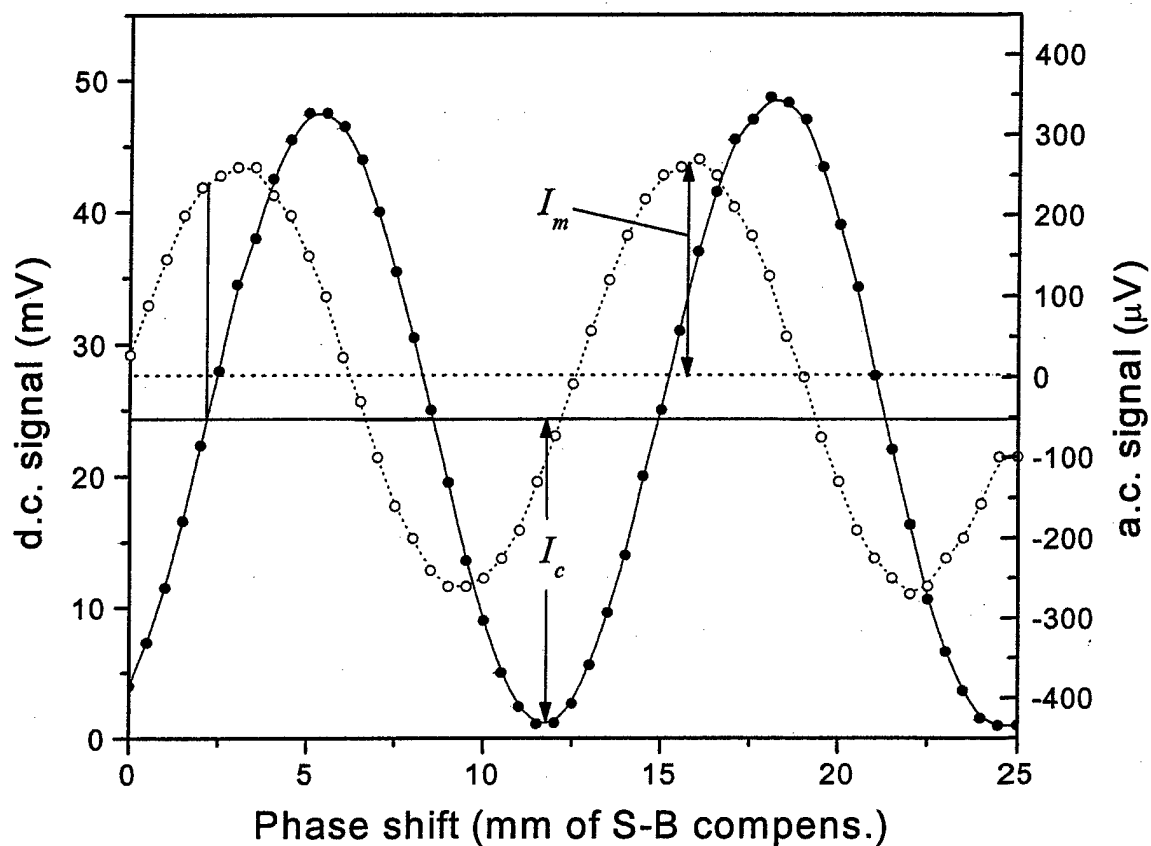


Figure 35. Experimental data related to the E-O effect in  $\text{LiNbO}_3$  sample studied with the experimental setup presented in Fig. 34. Solid line represents d.c. intensity versus the position of the micrometric screw of the Soleil-Babinet compensator (proportional to actual phase shift between horizontally and vertically polarized components of the incoming elliptically polarized light). Dotted line represents the amplitude of modulated light versus the position of the screw of the compensator.

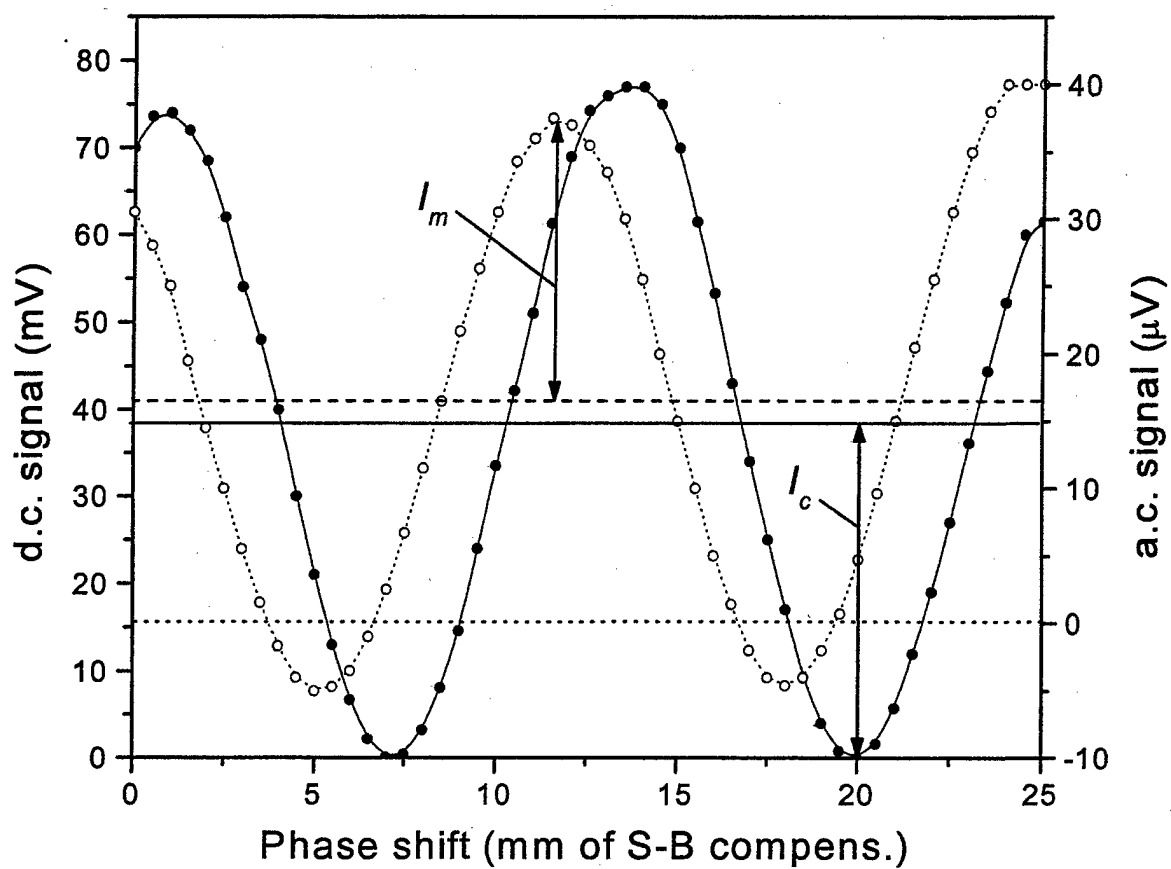


Figure 36. Experimental data related to the E-O effect in LD-3 polymer sample studied with the experimental setup presented in Figure 34. The designation of the lines is the same as in Figure 35.

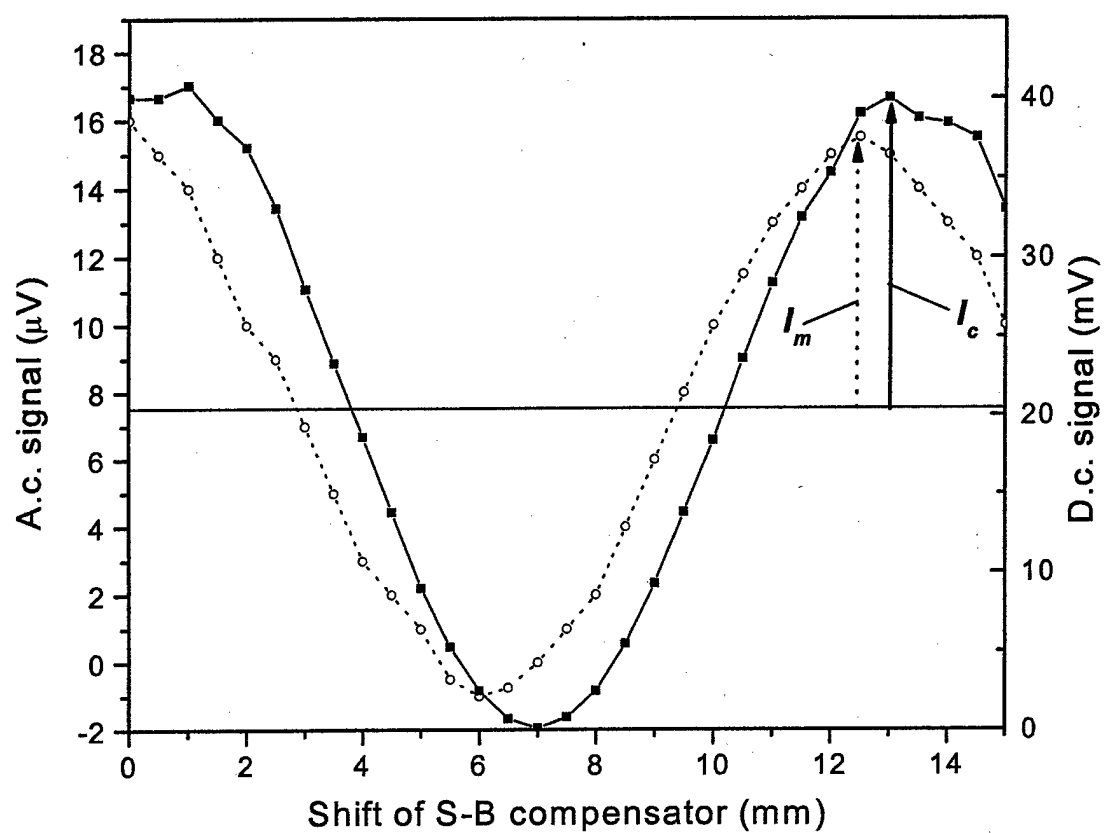


Figure 37. Experimental data related to the E-O effect in polyimide (synthesized by Dr. Connie Walton at GSU) sample studied with the experimental setup presented in Figure 34. The designation of the lines is the same as in Figure 35.

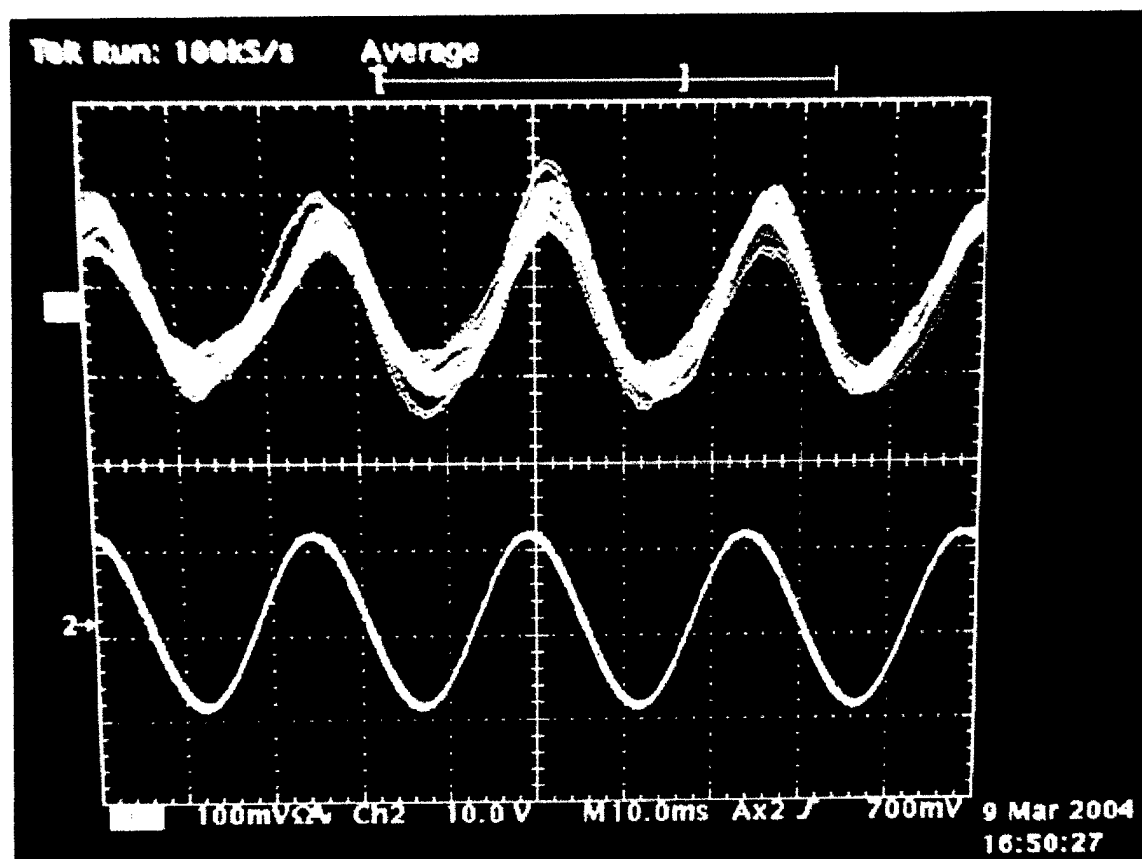


Figure 37. The oscillogram of the signal proportional to the varying intensity of light reflected from the film of poled polyimide from GSU (top) and the alternating voltage applied to it (bottom).

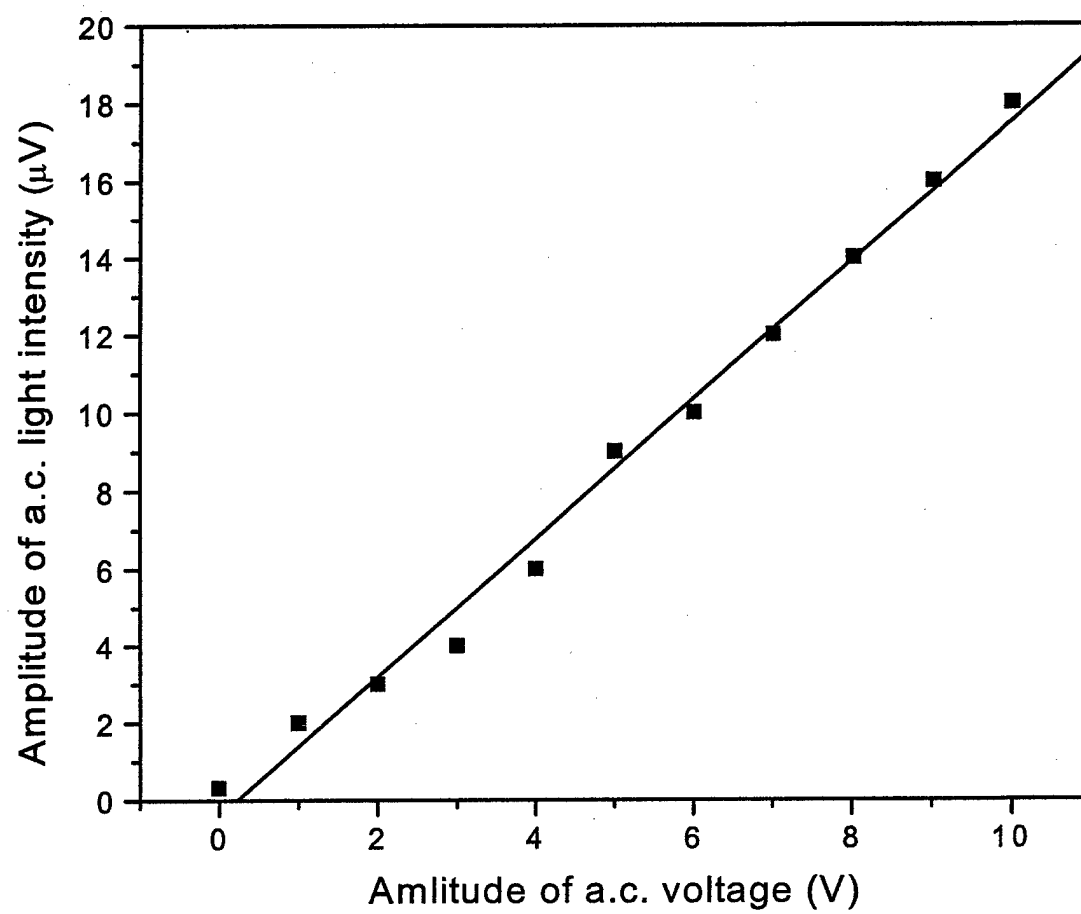


Figure 39. Amplitude of the modulation signal from the E-O polyimide film versus amplitude of the alternating voltage in (a) linear and (b) log-log scale.

## References

1. B. Furniss, A. Hannaford, P. Smith, and A. Tatchell (Editors). 1989. Vogel's Textbook of Practical Organic Chemistry. Essex England: Longman Publishing Company.
2. L.G. Wade. 2003. Organic Chemistry. New Jersey: Prentice Hall Publishing Company.
3. J. Scanlon, Journal of American Chemical Society, **57**, 887 (1935)
4. T.M. Moy, C.D. DePorter, and J.E. McGrath, Polymer, **34** (Number 4), 819 (1993)
5. C.C. Teng and H.T. Man, Simple reflection technique for measuring the electro-optic coefficient of poled polymers, Appl. Phys. Lett. **56**, 1734-1736 (1990).
6. A.M. Prokhorov and Yu. S. Kuz'minov, Physics and chemistry of crystalline lithium niobate, Adam Hilger, Bristol, 1990.
7. [www.adtechsystems.com/chemical.html](http://www.adtechsystems.com/chemical.html)

### **Part III**

#### **Presentations/Publications and Students/Staff Directly Involved with Project**

##### ***Grambling State University Student Presentations***

###### ***Natalie Arnett***

Title of Presentation: Synthesis and Characterization of Polyimides to be used in the Fabrication of a Low Driving Voltage Electro-Optic Modulator.

Presented at: 77<sup>th</sup> Annual Meeting of Louisiana Academy of Sciences Meeting, March 20-21, 2003, Gonzales LA.

###### ***Natalie Arnett***

Title of Presentation: Synthesis and Characterization of Polyimides to be used in the Fabrication of a Low Driving Voltage Electro-Optic Modulator.

Presented at: 13<sup>th</sup> Annual Phillip L. Young Research Symposium, April 29, 2003, Grambling State University, Grambling LA

###### ***Alex Lodge***

Title of Presentation: Synthesis of Polyimides that exhibit NLO Behavior.

Presented at: 7<sup>th</sup> Annual DOE-LAMP Conference, November 2003, New Orleans LA.

##### ***Presentations Given By Dr. Connie Walton***

Title: Synthesis of a Fluorene Polyimide

Presented at: Grambling State University, Chemistry Seminar Series, Spring 2002, Grambling LA.

Title: Synthesis and Characterization of Polyimides for Use in a Low Driving Electro-Optic Modulator.

Presented at: 59<sup>th</sup> Southwest Regional Meeting of the American Chemical Society, October 28, 2003, Oklahoma City OK.

Title: Overview of Scientific Research Being Conducted at Grambling State University.

Presented at: 2003 University of Southern Mississippi Undergraduate Research Experience Exchange Conference, March 3, 2003, Hattiesburg MS.

##### ***GSU STUDENTS WHO WORKED ON THIS PROJECT***

Natalie Arnett, Chemistry Major graduated Spring 2003, Currently 1<sup>st</sup> year graduate student in Chemistry at Virginia Tech.

Jamesha Wills, Chemistry Major in Junior Year at Grambling State University.

Alex Lodge, Chemistry Major in Sophomore Year at Grambling State University.

Claudia Tate, Former Chemistry Major, Transferred to another school

Penney Brown, Chemistry Major in Freshman Year at Grambling State University

Justin Henry, Chemistry Major in Freshman Year at Grambling State University

Ernest Anye, Computer Science Major at Grambling State University, Graduated December 2003

Yvette Thompson, Graduate Student

Joyce Ohene, Graduate Student

Natasha Jones, Graduate Student

### ***Publications***

Sergey S. Sarkisov, Connie Walton, Michael J. Curley, Leonid Yarovoi, J.\_C. Wang, "Electro-optic modulators based on high-temperature polyimides", in Proceedings of SPIE Vol. 4991 *Organic Photonic Materials and Devices V*, edited by James G. Grote, Toshikuni Kaino, (SPIE, Bellingham, WA, 2003) 589-600.

### ***Alabama A&M University Students & Staff Who Worked on This Project***

Faculty and staff at the Department of Physics, AAMU

1. Dr. Sergey S. Sarkisov, PI of the Sub-contract
2. Dr. Michael Curley

Students:

1. Aisha Fields, Ph.D. student, Physics (Applied Optics)
2. Burl Peterson, Ph.D. student, Physics (Applied Optics)
3. Courtney Boykin, M.S. student, Physics (Applied Optics)